A fluid inclusions study of Puerto Rico Tertiary dolomite

By:

María del C. Torres Vega

A thesis submitted in partial fulfillment of the requirements for the degree of

MASTER OF SCIENCE
in
GEOLOGY

UNIVERSITY OF PUERTO RICO
MAYAGÜEZ CAMPUS
December 2009

Approved by

_____	_____
Wilson R. Ramírez, Ph.D.	Date
President, Graduate Committee	
_____	_____
Hernán Santos, Ph.D.	Date
Member, Graduate Committee	
_____	_____
Clark Sherman, Ph.D.	Date
Member, Graduate Committee	
_____	_____
Samuel Santana, Ph.D.	Date
Representative of Graduate Studies	
_____	_____
Fernando Gilbes Santaella, Ph.D.	Date
Director of the Department of Geology	

Abstract

The north coast Tertiary limestone of Puerto Rico is composed of carbonate rocks that contain the most important aquifer in Puerto Rico. The dolomites of the north coast of Puerto Rico have been studied by González and Ruiz, (1991) by Ramírez, (2000). Both studies suggest mixing zone dolomitization for these dolomites. This study is based on the study of fluid inclusions analysis in the Puerto Rico north coast dolomites to better constrain in environment of precipitation. Fluid inclusions analysis provides direct information on the environments and the temperatures of precipitation. The samples of dolomites analyzed are from the Montebello Member at the Cibao Formations and the Lares Limestone. The temperatures obtained for the fluid inclusions present in Montebello Member at Cibao Formation at depth (510.1) and (420.1) are 0.0 and 0.1 at depth (510.1) that show a small quantity of salt in the samples. Fluid inclusions can be trapped during the process of recrystalization in diagenetic minerals. The inclusions that are present during the process of recrystallization provide the record of the conditions of recrystallization rather that the original precipitation of the mineral. The inclusions in north coast of Puerto Rico indicated the alterations of dolomites in fresh water environments and small quantity of salts zone where the dolomites have been precipitated meteoric-marine mixing zone. Stable isotopic analysis in the same samples was made to help identify the environments of precipitation. The stable isotopic analysis in Garrochales at Barceloneta Quadrangle, Manatí Quadrangle and Lares Limestone and Montebello Member at the Cibao Formation cores indicated alterations in meteoric and marine water.

RESUMEN

La costa norte de Puerto Rico en su gran mayoría está compuesta por carbonato de calcio y contiene el sistema de acuíferos más importantes de Puerto Rico. La estratigrafía de la costa norte de Puerto Rico ha sido estudiada por varios autores durante los últimos años. Los únicos estudios específicos en las dolomitas de la Costa Norte de Puerto Rico han sido Gonzáles y Ruiz (1991) y Ramírez, 2000. Ambos estudios determinaron que las dolomitas de la costa norte habían sido precipitadas en ambientes de zonas de mezcla de agua meteórica y agua marina. Este estudio se basa en determinar el ambiente de dolomitización mediante la técnica de análisis de inclusiones de fluidos (fluid inclusion análisis) que provee información directa sobre el ambiente y la temperatura precipitación las dolomitas de la costa norte de Puerto Rico. Las inclusiones de fluidos de la Montebello Member at Cibao Formation a la profundidad de (420.1m) y (510.1) fueron de 0.0 indicando área de zonas de agua fresca y el dato de 0.1 indica pequeñas cantidades de sal en la muestra. Las inclusiones de fluidos que aparecen duran el proceso de recristalización proveen el record y el ambiente del procesos de recristalización y no del ambiente original. Esto sugiere que las inclusiones representan alteración en ambientes meteóricos Para determinar y comparar la data obtenida por las inclusiones de fluido también se llevaron a cabo estudios de isótopos estables. Muestras de los cores Garrochales, at Barceloneta Quadrangle, Manatí Quadrangle and Lares Limestone and Montebello Member at the Cibao Formation indicaron en que las dolomitas fueron alteradas o precipitadas en ambientes meteóricos y marinos.

Dedicado a mí hermano Francisco José por ser mi inspiración y mis pasos a seguir. Mis padres Francisco Torres y Carmen Vega por su apoyo y compresión........

Acknowledgements

Table of Contents

List of Figures

obtained suggest alteration of the Sr isotopic signatures in waters produced

by rock-water interaction in the host aquifer rocks, because the Sr isotopes

in the dolomites are very similar to the Sr isotopic values of the host rocks

were dolomitization occured. The Sr values obtained would imply that

dolomitization and deposition of the limestones occurred at the same time

and this is imposible especially for replacive dolomites as the ones studied 96

List of Tables Contents

Chapter 1

1.1 Introduction

The rocks of the north coast of Puerto Rico are composed of Tertiary Limestones. The stratigraphy of the north coast has been study by several authors (Ward et al., 2002). The dolomites have been studied by Ramírez (2000) and González and Ruiz (1991). Ramírez (2000) and González and Ruiz (1991) did geochemical, petrographic and isotopic analysis and proposed that these dolomites were formed in a mixing zone environment.

Using the fluid inclusions trapped in the dolomites, this study established how these dolomites formed. This technique show if the environment of dolomitization was in the mixing zone, seawater or freshwater and corroborate or contradict the previous authors assessments. This is the first time fluid inclusions are used in Puerto Rico to determine the environment of dolomitization of these dolomites. Using fluid inclusions and the previously obtained data by Ramírez (2000) and González and Ruiz (1991) a model for dolomitization in the north coast of Puerto Rico is proposed.

1.1.1 Motivation

The north coast of Puerto Rico has been studied by several investigators, including Hubbard (1923), Zapp et al., (1948), Meyerhoff (1975), Monroe (1980), Seigle and Moussa (1984), and Ward (2002) that studied and established the stratigraphy of the north coast of Puerto Rico. The north coast Tertiary Limestones contains the most important aquifers of Puerto Rico. The dolomites in the north coast Tertiary basin of Puerto Rico have been studied by Ramírez

(2000) in the Montebello Member of the Cibao Formation and the Lares Limestone and by González and Ruiz (1991) in the Aymamón Limestone. Due to the available petrological and geochemical methods at that time, a debate still exists about the formation of these dolomites and many others.

Fluid inclusions analysis is a relatively new technique that helps us to identify the specific fluid that precipitated the dolomites. The analysis was used in conjunction with the studies of Ramírez (2000) and González and Ruiz (1991). All the data available is used to make a better constrained model of dolomitization. A better constrained of the model of dolomitization is going to help us to determine and understand the geology of the north coast and the precipitation for the dolomite. The stable isotopes analysis is going to be used to determine is there is alteration or not in the dolomite samples. These data of stable isotopes is compared to the stable isotopes results of Ramirez (2000) to determine if there is alteration in the dolomites and the environments of precipitation. The data obtained here by the fluid inclusion analysis is important to determine, establish, and understand the environment of dolomitization.

1.1.2 Objectives

1. To study the fluid inclusions in the dolomites present in the Lares Limestone and Montebello Member of the Cibao Formation and to characterize the dolomitization fluids.

2. To compare the results obtained with the two previously proposed mechanisms for dolomitization along the north coast (Ramírez 2000, Machel 2000) and to determine which one, if any, is the most appropriate model:

2

a. Fluid inclusion analysis supports dolomitization by hydrothermal fluids as proposed by Machel (2000);

b. fluid inclusions analysis supports the mixing zone model of dolomitization by Ramírez (2000) and by González and Ruiz (1991);

c. the fluid inclusion analyses do not support any of the previous models and suggests other possibility.

1.1.3 Literature Review

There is little work done in the dolomites of the north coast of Puerto Rico and none using fluid inclusions analysis. Machel (2000) studied the dolomites in Barbados, Gran Cayman, Jamaica and St. Croix. His petrographic analysis suggested that the dolomites from all these locations are similar and formed at similar times. Machel (2000) proposed that the dolomites in the Caribbean formed by tectonic activity and hydrothermal solutions associated to it. These hydrothermal solutions are driven by magmatic heat for compressional margins dolomitization that occurred as results of chemical modified seawater cold or hydrothermal by the tectonics compressions (Machel, 2000).

The diagenesis study of the Aymamón Limestone done by González and Ruiz (1991) was based in geochemistry, petrology and geological history of the area. The study was part of the Toa Baja well drilling project (Fig.1.1). They proposed meteoric-marine mixing zone environments for dolomitization with the process of dolomitization as one of the latest events in the paragenetic sequence. This event probably occurred during a major marine offlap that produced the extensive erosional unconformity on top of the Aymamón Limestone (Monroe,

3

1980a), or during the submergence of the Aymamón Limestones in times of deposition of the Quebradillas Limestones in the Pliocene (Moussa et al., 1987).

Ramírez (2000) evaluated the dolomites present in the north coast of Puerto Rico. Different cores along the north coast of Puerto Rico were studied including their petrography, isotopic and geochemical analysis, and the study of the geological history of the area. The data obtained suggest that the sea level rise during the Miocene produced the conditions for dolomite to precipitate in a mixing zone environment. Ramírez (2000) proposed that most dolomites in the Montebello Member of the Cibao Formations and Lares Limestone formed in a mixing zone of marine and phreatic water in a confined aquifer system. The subsurface and down dip location of the dolomite, in these two units, suggests that dolomitization in the Lares Limestone and the Montebello Member of the Cibao Formations was constrained to the subsurface.

TOA BAJA WELL #1
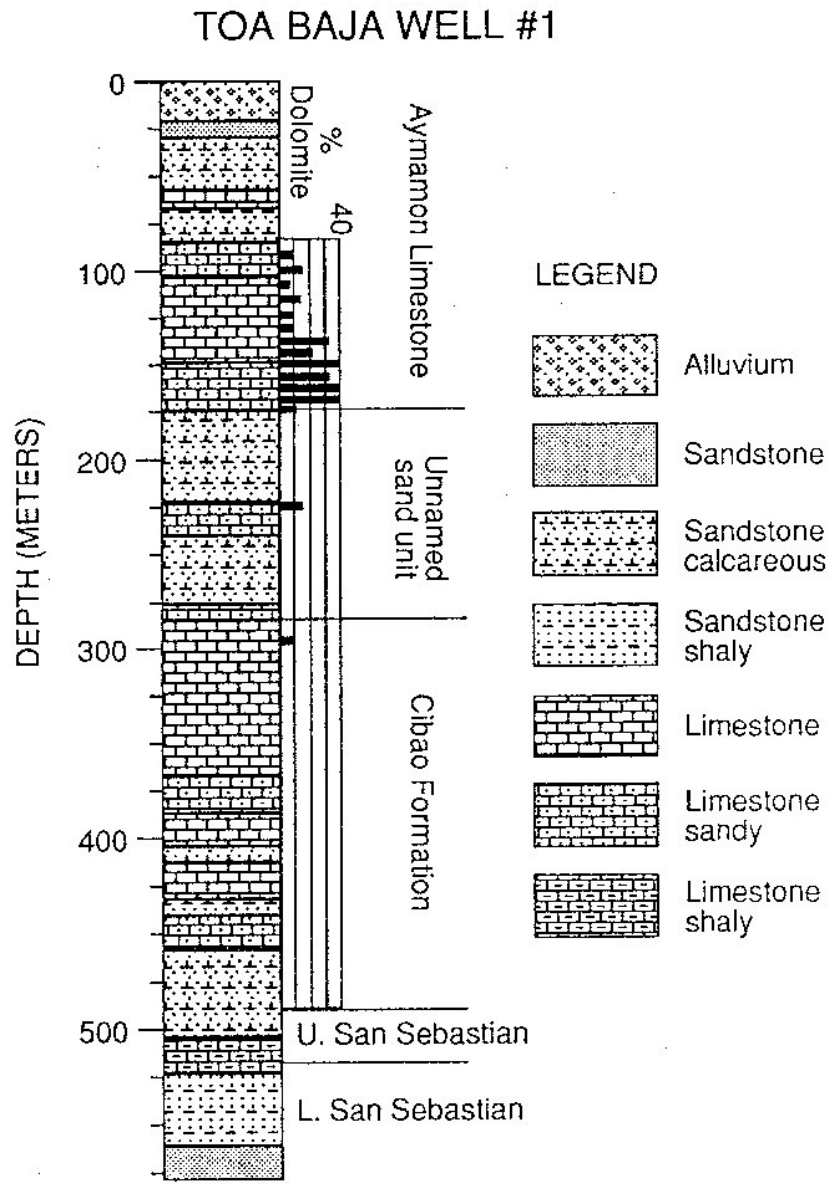
Figure 1.1: Stratigrahy of the Toa Baja #1 Well. Formations were established by Montgomery et al., (1991) and González and Ruiz, (1991).

1.2 General Geology and Stratigraphy

1.2.1 Introduction

The north coast Tertiary limestones of Puerto Rico were studied in 1986 by the United States Geological Survey (U.S.G.S.). They studied the aquifers of the north coast by doing core drilling. The data obtained also provided information of the lithostratigraphy and stratigraphic sequence of these limestones. They suggested that the limestones along the north coast were deposited in a shallow water stable shelf. Most investigations consider that the limestone was deposited during Oligocene to Middle Miocene age (Giusti, 1978).

1.2.2 Tectonic Setting of Puerto Rico

The island of Puerto Rico contains extensional and compression elements and strike-slip movements (Mann et al., 1998; DeMets et al., 2000; Bilich et al., 2001; McCann, 2002; Prentice et al.,2003) (Figure 1.2). In the Caribbean most of events occurred by; continental margin magmatism in association with the break of Pangea. The north and South American plates spread apart about 140 million years ago. The subduction of the Pro-Caribbean formed the Caribbean Plate (Mattson, 1984).

An uplift in the southern portion of the north Tertiary basin occurred and the rest of the northern Tertiary platform was tilted to the north and subducted. Birch (1986) proposed that the subsidence in the north coast of Puerto Rico occurred in stages. The first stage occurred during the Eocene to Mid-Oligocene and consisted in tensional thinning causing and uniform subsidence. The second stage occurred during the Oligocene to Miocene when the area sank almost 2 km due to sediment loading and thermal contraction form the magmatism in the

previous stage. The last stage occurred during the middle Pliocene when the Caribbean started subduction under the North America plate for the the second time.

Birch (1986) suggested that these subduction episodes caused hundreds of meter of uplift in the southern portion of the north Tertiary basin; the rest of the northern Tertiary platform was tilted to the north and subducted.

The eustatic-sea-level during the Oligocene-earliest Miocene is represented in northern coast plain of Puerto Rico by San Sebastian-Lares mudstones unit sequences (terrestrial to outer platform deposits) (Scharlach, 1990).

The period of eustatic sea level rise during the Oligocene between 22 mya and 24.9 mya middle-shelf (Lares Limestone) deposition in the central northern Puerto Rico eventually gave way to relatively deep-water deposition (Mudstone Unit). The Cibao Formation is more related to 10.5-21 mya period. The inner platform and marginal marine sedimentation occurred during the lowstand in sea level (17.6-21 mya) (Scharlach, 1990).
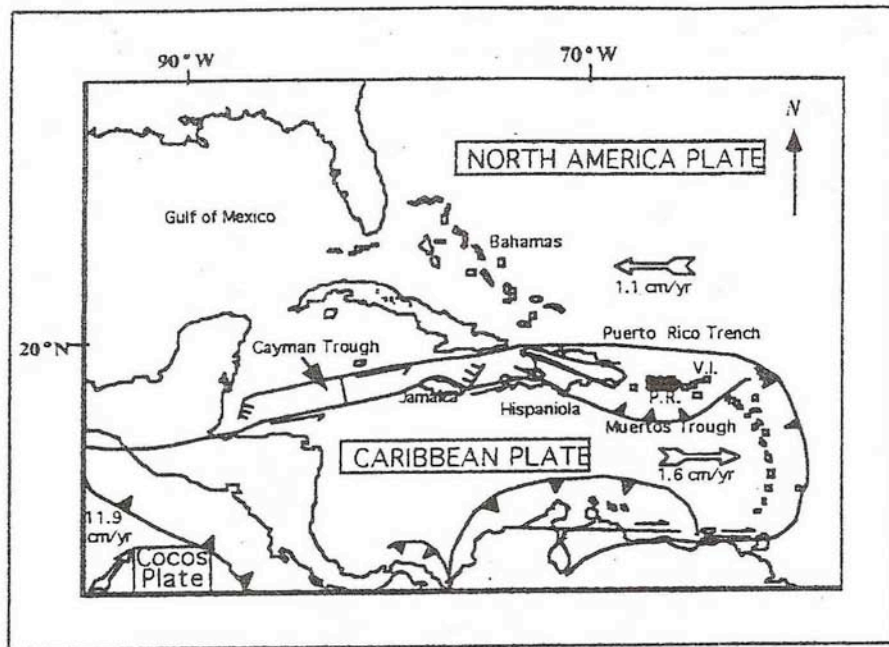
Figure 1.2: Tectonic map of the Caribbean and plate motion velocities
(from Mann *et al*.,1984).

1.2.3 Previous Investigations

Berkey (1915, 1919) divided the sedimentary sequences in the north coast of Puerto Rico into the San Sebastian Shale and the Arecibo Formation. Hubbard (1923) further divided the middle Tertiary rocks into; the San Sebastian Formation, the Lares Limestone, the Cibao Formation, the Los Puertos Formation and the Quebradillas Limestone. Zapp et al. (1948) divided the rocks younger than the Cibao Formation into the Aguada and Aymamon Limestone. Meyerhoff (1975) study the base of the Aguada Limestone and Los Puertos Limestone and concluded that these two formations represent the same units (Fig. 1.3). Meyerhoff et al. (1983) and Seigle and Moussa (1984) described an unconformity between the Los Puertos Limestone (Aguada Limestone) and the Aymamon Limestone.

Seigle and Moussa (1975) and Meyerhoff (1975) argued that the Camuy Formation of Monroe (1963a) is essentially similar to the Quebradillas Limestone of Hubbard (1923) (Fig. 1.3). Meyerhoff et al., (1983), Seigle and Moussa (1984) described and unconformity between Los Puertos Formation (Aguada Limestone) and Aymamon Limestone. Meyerhoff et al., (1983) designated the unit above this unconformity as the Moca Formation (Fig. 1.3). The Moca Formation has not been defined but the name of Aymamon Limestones is used for the unit between Los Puertos Limestone (Aguada Limestone) and the Quebradillas Limestone. Seigle and Moussa (1975) argued that the Quebradillas Limestone is thicker and suggested that the Camuy Formation and the Quebradillas Limestone are essentially equivalent. They renamed the Camuy Formation into the Quebradillas Limestone.

The stratigraphic nomenclature used for this study is that of Renken et al., (2002) (Fig. 1.3). This stratigraphic nomenclature is the one used by the U.S.G.S. The statigraphic divisions are, in ascending order: the San Sebastian Formation, the Lares Limestone, the Cibao Formation, the Aguada (Los Puertos) Limestone, the Aymamon (Moca) Limestone, and the Quebradillas (Camuy) Limestone. Toward the east the Lares Limestone and the Cibao Formation interfinger with the Mucarabones Sandstone. This investigation will be focused in the Lares Limestone and the Montebello Member of the Cibao Formation dolomitic rocks.

AGE		Hubbard, 1923	Zapp and others, 1948	Meyerhoff, 1975	Monroe, 1980	Seiglie and Moussa, 1984	This report (subsurface)
PLIOCENE						Quebradillas Limestone	Quebradillas Limestone
MIOCENE	LATE			Quebradillas Limestone	Camuy Limestone		
	MIDDLE			Los Puertos Limestone		Aymamòn Limestone	Aymamón Limestone
						Los Puertos Limestone	Aguada (Los Puertos) Limestone
	EARLY		Aymamón Limestone		Aymamón Limestone	Cibao Formation	Undifferentiated Cibao Formation
			Aguada Limestone		Aguada Limestone		Montebello Limestone Member / Mudstone unit / Quebrada Arenas and Rio Indio Limestone Members / Mucarabones Sand
				Cibao Formation	Cibao Formation	Montebello Limestone / Mudstone unit	
					Mucarabones Sand		
OLIGOCENE	LATE	Quebradillas Limestone	Cibao marl	Lares Limestone	Lares Limestone	Lares Limestone	Lares Limestone
		Los Puertos Limestone					
	"MIDDLE"	Cibao Limestone	Lares Limestone	San Sebastián Formation	San Sebastián Formation	?	San Sebastián Formation
		Lares Formation				San Sebastián Formation	
		San Sebastián Shale	San Sebastián Formation				

Figure 1.3: Stratigraphic nomenclature evolution of Oligocene, Miocene and Pliocene sedimentary rocks of the north coast Tertiary basin of Puerto Rico (from Ward et al., 2002).

11

1.2.4 The Lares Limestone

A major rise in sea level began during the Late Oligocene. This rise in sea level was recorded by the gradation of shallow marine deposits of the Upper San Sebastian Formation into the inner to midplatform carbonate and terrigeneous deposits of the lower Lares Limestone (Hartley 1989). The middle part of the Lares Limestone records a maximum transgression of the late Oligocene sea. The soritid and miliolid rich limestones of the uppermost Lares Limestone indicate that inner- to middle-platform environments spread seaward over much of the early material. Hartley (1989) explained that the middle Lares Limestone formed in shallow-marine environments and that the upper Lares Limestone represents a near-shore environment. Hubbard (1970) defined the Lares Limestone as a massive limestone overlying the San Sebastian Formation. The Lares Limestone was deposited in a 25 km shelf rich of marine organisms that were similar to the modern reef environments. The eastern and western boundaries of the basin during the Lares Limestone time are formed by fluvial deposits (Monroe 1980a).

1.2.5 The Cibao Formation

The Cibao Formation has a heterogeneous lithology and it is stratigraphically located in the middle of the Tertiary Formation of Puerto Rico. The Cibao Formation was deposited during the Late Miocene. The Cibao Formation was described by Hubbard in 1923. Monroe (1980) concluded that the Cibao Formations was deposited by different environments, including fluvial, deltaic, nearshore (clastic) and marine (carbonate). Frost et al., (1983) described that the Cibao Formations in the central part of Puerto Rico as a marginal-marine to marine mudstone, marl and limestone.

The upper part of the Cibao Formations is composed of sandstones and sandy limestone. Hartley (1989) notes similar occurrences in the Cibao Formation in the west of the basin and concluded that influx of coarse detritus indicates a sea-level drop or basin-wide tectonic uplift and the end of the Cibao Formation deposition.

The Cibao Formation is composed of clastic material that is found between the Lares Limestone and the Aguada Limestone. The Cibao Formation is one of the most heterogeneous and lenticular of the Middle Tertiary formations in northern Puerto Rico. It is composed of interlensing beds of calcareous clay, sandy clay, and intergradational sand and gravel. The Cibao Formation in Camuy contains beds of marls with abundant oyster shells and beds of pink or white limestones with *Lepidocyclina* and *Orbilotites*.

1.2.5 The Montebello Member of the Cibao Formations

The Montebello Member of the Cibao Formation is composed of skeletal and foraminiferal packstones and wackestones, and dolomites. The Montebello Member, in east to west direction, represents the marly limestones of the Cibao Formations (Monroe, 1980; Meyerhoff, 1983). Frost et al. (1983) studied the Montebello Member near the town of Lares and described the basal part to be molluscks-rich packstones and graintones overlain by a sequence of interbedded wackestones and packstone (Scharlach, 1990).

1.2.6 Description of cores

The U.S.G.S., starting in 1984, did many investigations of the aquifers of the north coast Tertiary Limestones of Puerto Rico. This project was done to evaluate the lithological and hydrological characters of the limestone, delineate the geographical extension of the lower artesian aquifers, describe the water quality and characterize water bearing units (Renken, 2000). The project consisted of drilling the limestone to obtain the subsurface information. This study focuses on dolomite samples from the Montebello Member of the Cibao Formation and Lares Limestone present in the following cores Garrochales, IAS-4, IAS-1, NC-5, NC-6, NC-9 and NC-10 (Fig. 1.4).

The Montebello member was penetrated by the cores NC-5, NC-6 and NC-10 (Sharlach, 1990). The core NC-5, in the Barceloneta Quadrangle, has a depth of 387.8 m. The Montebello Member in the Barceloneta Quadrangle is composed of yellow to very-pale orange, fine to medium grained packstones-grainstones. The lower part the section is dolomitic. Foraminifers are dominant with echinoderms, pelleoids and molluscks that include some gastropods and kuphus (Hartley, 1989). In the NC-6 core the Cibao Formation occur at 707.6 m. This core is composed of light-green-gray calcareous claystones topped with a few wackestones that contain oysters and blackened clasts (Hartley, 1989).

The Montebello Member of the Cibao Formation samples in core IAS-4 is located at IAS4-(590.5), IAS4-(563.1m), IAS4-(510.1 m), IAS-4 (556.6m), IAS-4 (461.3m), and IAS-4 (420.1m). Here this formation is part of the inner shelf environment and is interbedded with shales. The benthic foraminifers *Amphistegina*, and *Lepidocyclina*, rotalids, echinoids, bivalves, Kuphus and ostracods are present (Ramírez, 2000).

The samples studied in the NC-9 core were collected at the depths of NC-9 (477.4 m), NC-9 (520.7 m) and NC-9 (525.3 m). The NC-9 core in the Manatí Quadrangle did not penetrated the lower part of the Cibao Formation (Scharlach, 1990). The formations present in the core are the Aymamón Limestone, the Los Puertos Formation and the Cibao Formation. The samples studied are at depths of NC-9 (477.4 m), NC-9 (493.0 m), and NC-9 (525.3 m).

The NC-10 core reached 430.8 m in depth. This core is in the Barceloneta Quadrangle. The Montebello Member of the Cibao Formation is present in the core and is composed of a "shoaling upward" sequences that are developed in the NC-10 core (Scharlach, 1990). These samples have pale-orange to very pale-orange sucrosic dolomite, red algae wackestone, and mollusks, *Halimeda* and dasyclad algae, ostracodes, and echinoderms. Intraclast of pelleoidal wackestone, packstone, algal laminations and fenestral fabric are also found. The dolomite samples are present associated with red algae and mollusks (Scharlach, 1990).

The core IAS-1 is located at the Manatí Quadrangle and only the Lares Limestone was sampled. Samples are located at IAS1 (477.4 m), IAS1 (679.9 m) and IAS1 (612.8 m). The intervals IAS1 (685.9 m) to IAS1 (731.7 m) are composed of dolomite and bears red algae, *Lepidocyclina*, soritids and other foraminifers, echinoids, small benthic foraminifers, mollusks and some corals. The interval from IAS1 (612.8 m) and IAS1 (681.4 m) is composed of coarse-grained packstones and lesser graintones and contains plantonic foraminifers. The upper parts of this interval are composed of quartz, lithic sand and glauconite (Scharlach, 1990). These intervals were deposited in low energy mid-platform environments and represent deep water deposits. They have some rhodolith banks and a few coral algal biostromes.

The Garrochales core is in the Barceloneta Quadrangle. The samples studied in the core are at the following; depth Garr (636.3 m), Garr (653.0 m), Garr (714.0 m), Garr (718.2 m), Garr

(485.6 m), Garr (498.1 m), Garr (522.9 m), Garr (530.2 m), Garr (587.6 m) and Garr- (655.5 m). This core shows a middle shelf to seaward open marine moderate to high wave energy environment. The foraminifers present in these cores are *Lepidocyclina*, *Amphistegina*, other fossil are red algae, and coral boundstones, skeletal wackestones, packstones and shale are present. The depositional environments are mostly dominated by normal salinity biota that includes echinoids, massive and branching corals, gastropods, rhodolites, articulate red algae and milliolids.
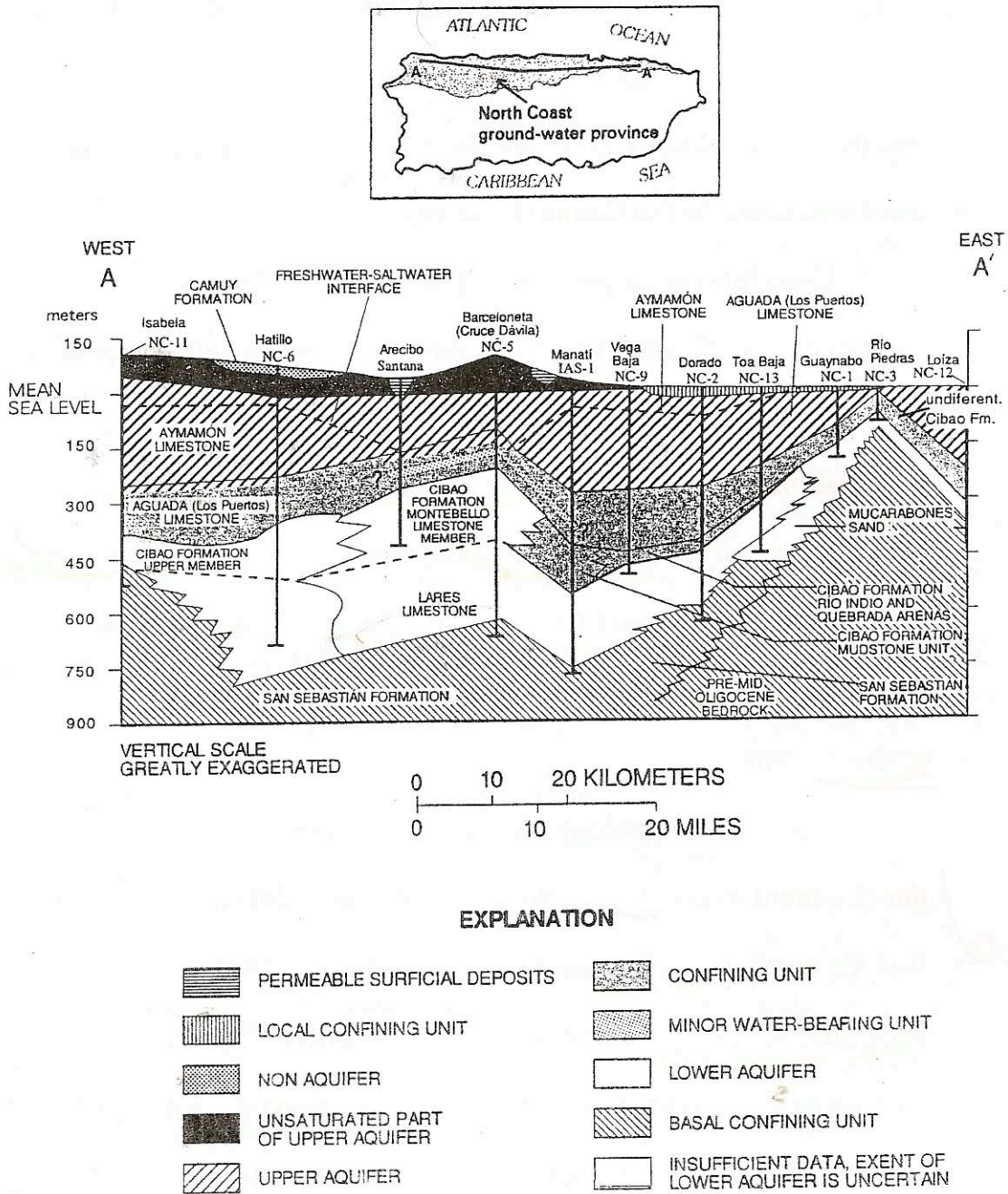
Figure 1.4: Cross section (A-A') of the hydrogeology of northern Puerto Rico (from Rodríguez Martínez, 1995).

17
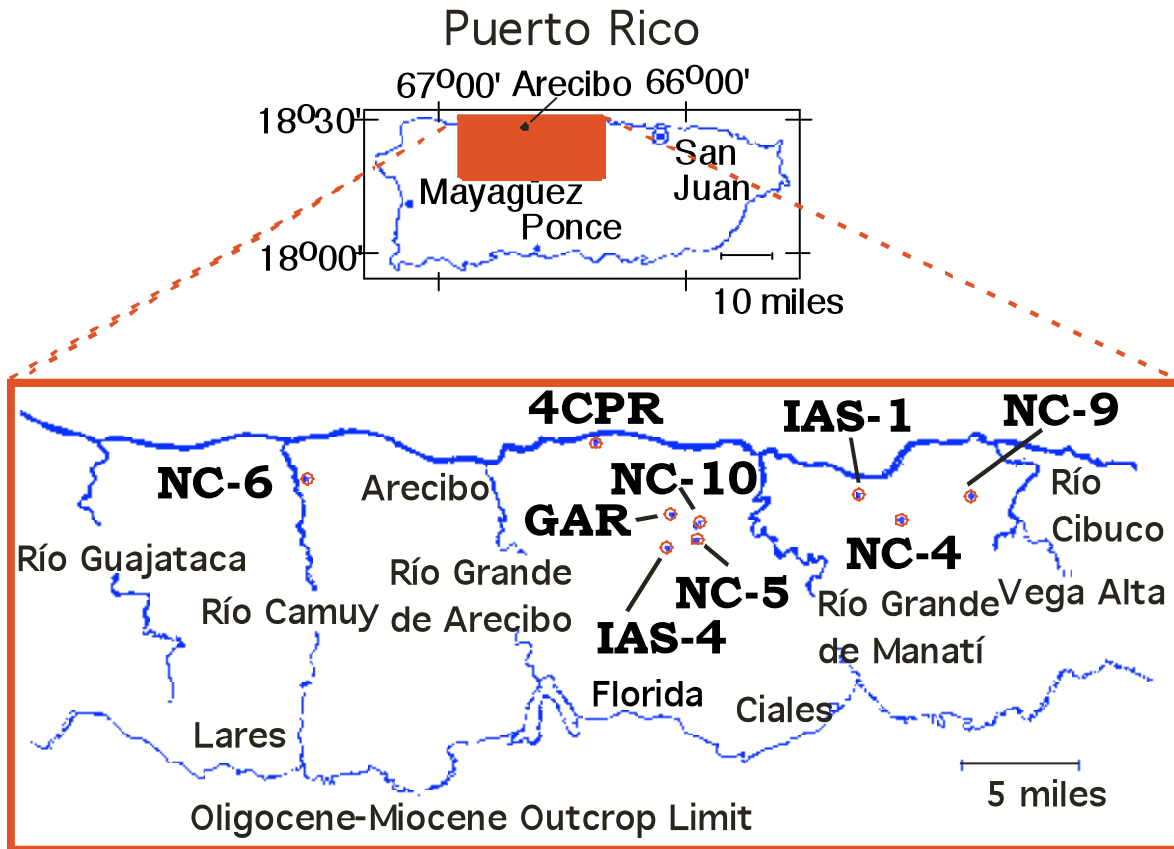
Figure 1.5: Location of the U.S.G.S. cores that contain the samples of dolomites and are examined for the north coast of Puerto Rico

1.3 Hydrology of the north coast of Puerto Rico

1.3.1 Introduction

The most extensive aquifers of the U.S. Caribbean Islands are located in the North coast of Puerto Rico. This aquifer system is divided into four different hydrologic units, an upper unconfined aquifer, a middle confining unit, a lower artesian aquifer, and a basal confining unit (Rodríguez-Martínez, 1995; Renken et al., 2002).

The artesian aquifer occurs in the Lares Limestone and the Montebello Limestone Member of the Cibao Formation. The Montebello Member is composed of chalky limestone (Guisti, 1978). The petrography, geologic history and stratigraphy of the rocks is important in the determination of the dolomitization environments, in (marine, fresh water or mixing zone environments). According to (Guisti, 1978) these aquifers formed during the Miocene due tectonically related uplift and tilting of the carbonate units during the late Miocene. The eustatic sea level drop, and also tilting and uplift exposed the Lares Limestone and the Montebello Member of the Cibao Formation units along an extensive area. These uplift provided a meteoric recharge area and a high potentioemetric gradient in the previously marine phreatic environments allowing meteoric waters to invade the carbonate units to form freshwater phreatic conditions and to form the aquifers (Guisti, 1978).

The other important aquifer that occurs in the north coast Limestones is a water table aquifer in the Aguada and Aymamón Limestone and in alluvial deposits (Román and Lee, 1987). The areas of the artesian aquifer that are unconfined are referred to as lower aquifer instead of artesian aquifer in the U.S Geological Survey (e.g. Rodríguez-Martínez, 1995). The artesian aquifer and water-table aquifer are separated by a confining layer of chalky marly material within the upper part of the Cibao Formation (Monroe, 1980). The water that enters in the

system moves northward. The upper part of the Cibao Formation forms a low permeability zone at the base of the aquitard. The freshwater progressively moved down dip and occurred under artesian conditions near the coast (Román and Lee, 1987). Salty connate water originally occupied the Limestones.

The Cibao Formation is an extensive formation that covers the north coast of Puerto Rico and is composed by these members; the Montebello Limestone Member, the unnamed mudstone unit and the unnamed upper part called the Quebradas Arenas Member (Guisti, 1978 and Matos, 2000). The mudstone unit is composed of deep water claystones and marls (Matos, 2000). The dolomite zones occur in the upper and lower parts of the formations (Ward and Hartley, 1985). This formation occur as part of a confining bed or as an aquifer. The underlying Montebello Member of the Cibao Formation is composed of thick-bedded to massively finely crystalline to granular Limestone. The two formations in the lower artesian aquifer probably occur in confined and unconfined conditions depending of the geographical position. The Quebrada Arenas Formation is present in the middle of the belt (Rodríguez-Martínez, 1995). The Montebello Member of the Cibao Formation is an important artesian aquifer in the middle part of the limestone units (Ward and Hartley, 1985).

Three different theories that explain the times of exposure of the Lares Limestone and Montebello Member were proposed by Renken, (2002). The first two theories proposed that the time of exposure occurred during the early and middle Miocene. During the geological settings these units were characterized by a gently dipping carbonate platform. The low inclination on the units and their proximity to sea level did not produced the "potentiometric strength" needed for the meteoric water to displace the dense particles of marine or connote water from thee carbonate rocks (Renken, 2002).

The third possibility of exposure was present in the late Miocene (Renken et al., 2002). At this time the relative significant sea level drop was recorded by the unconformity that exists between the Quebradillas and Aymamón Limestones (Ramírez, 2000). This relative sea level drop was caused by the tilting of the north coast Limestones. The events of uplift, tilting and sea level drop provided the hydraulic gradient needed for the meteoric water to flush out the marine waters present in the limestones.

1.4 Dolomitization

1.4.1 Introduction

Dolomite is a rhombohedral carbonate that is composed of magnesium calcium carbonate, $CaMg(CO_3)_2$. Dolomites are sedimentary rocks that can be precipitated from seawater but do not have an even distribution through the time (Tucker and Wright, 1990). Commonly these rocks are porous and hence represent a target for petroleum exploration and a host for sulphide mineralization. Dolomite is difficult to precipitate in laboratory experiments because the mineral is highly ordered and requires time to precipitate (Tucker and Wright, 1990).

Dolomites are found in the Late Oligocene through the Lower Miocene Limestone section along northern Puerto Rico and provide the opportunity to study the aquifer system.

Seawater is supersaturated with respect the dolomite, but dolomite does not precipitates in normal marine environments. Modern dolomites were discovered in the late 1950s and early 1960s (Tucker and Wright, 1990). A factor that promotes the formation of dolomite is a high concentration of Mg^{+2} ions combined with movement of dolomitization fluid through the carbonates sediments. There are five different models of dolomitization: 1) evaporative; 2) seepage-reflux; 3) mixing zone; 4) burial; and 5) seawater models (Fig.1.6).

If dolomitization occur in limestone, three requirements must be met; a source of Mg^{2+} adequate to dolomitize the limestone, a transport mechanism to carry the Mg^{2+}, and the dolomitization fluid must be supersaturated with respect to dolomite.

An exposure of the dolomite is found at the top of the Lares Limestone in the road P.R. #111 (Soto, 2009 and Ortega, 2009). Monroe (1980a) described the lithology and stratigrahy of the Lares Limestone and he found that the formation is composed mostly of "calcium

carbonate". In the subsurface, dolomite is present in both the Lares Limestone and the Montebello Member of the Cibao Formation in most of the cores. The distribution of the dolomite changes in the different stratigraphic units. The Lares Limestone has dolomite in nearly all the core sections studied while the Montebello Member of the Cibao Formation is only partially dolomitic.
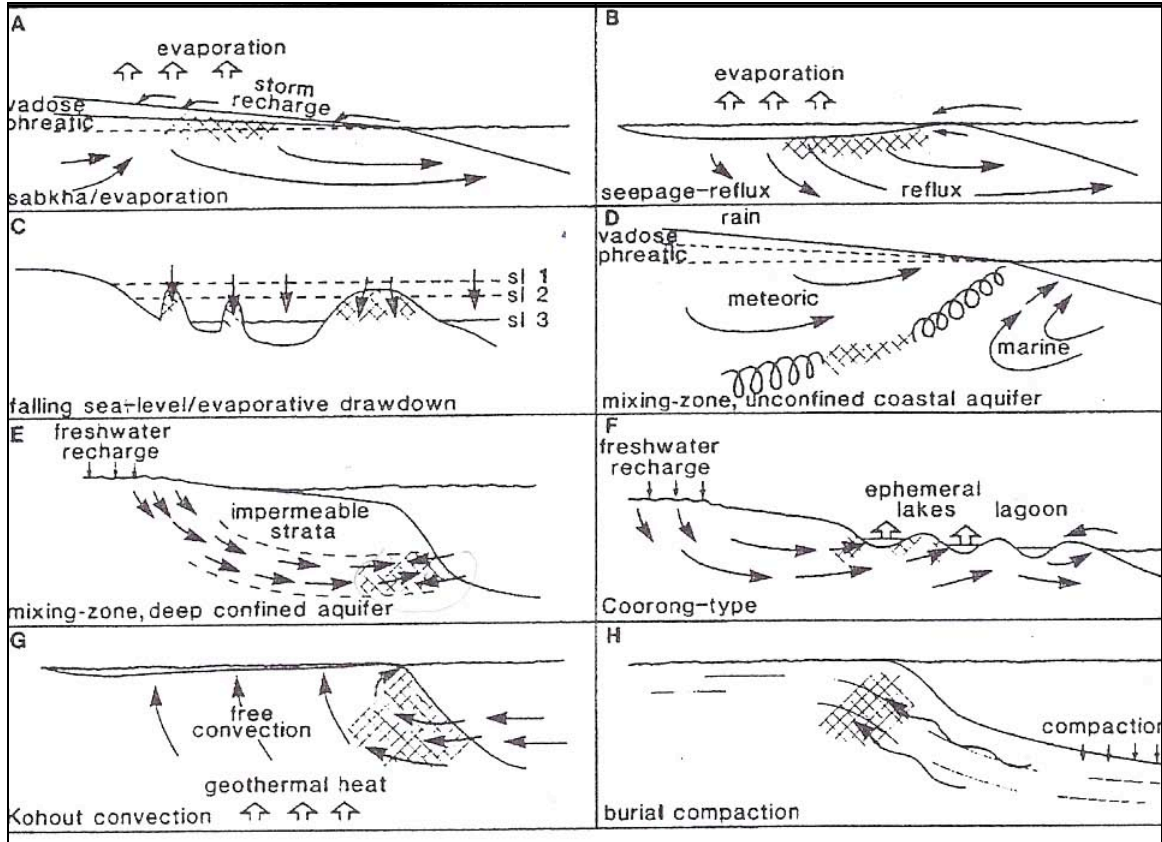
Figure 1.6: Models of dolomitization illustrating the mechanisms for
moving dolomitization fluids through the sediments
(Tucker and Wright, 1990).

1.4.2 Diagenesis

Most of the recent marine carbonate sediments are composed of aragonite, high Mg calcite and low- Mg calcite. Low-Mg calcite is a stable form of $CaCO_3$ and these cements are commonly precipitated from meteoric water in the near surface as well as from the basinal fluids (Tucker and Wright, 1990). Most ancient limestone deposits are composed of low-Mg Calcite.

1.4.3 Evaporative Dolomitization

The following minerals are common in the dolomitization evaporative model: gypsum, anhydrite and halite. These models involve the evaporitic environments forming sedimentary dolomites. The environment involves the periodic flooding into sediments, tidal pumping, and intense evaporation of water in the capillary zone that cause the "evaporative pumping". The replacement of aragonite and associated gypsum which raise the Mg/Ca ratio is involved in the formation of dolomites in evaporitic environments (Tucker and Wright, 1990). This model does not fit for the dolomites present in the Lares Limestone and the Montebello Member of the Cibao Formation because the minerals gypsum, anhydrite and halite are not present in any of the cores. In addition the geologic history does not support evaporation as a dominant process in this area during the time of dolomitization since data available suggest that the rocks were already in the sub-surface at the time of the dolomitization.

1.4.4 Seawater Dolomitization

Mg^{+2} sources for dolomitization from seawater are provided by pumping or inflow combined with buoyant rise of geothermal heated seawater at continental margins (Tucker and Wright, 1990). This model cannot explain the precipitation of dolomites in the north coast of Puerto Rico because the hydrologic units in the north coast do not show any evidence of free convection from deeper water units that are part of the confined aquifer system.

1.4.5 Mixing Zone Dolomitization

The dolomites in mixing zone are formed by a mixture of the seawater and freshwater that produces a zone that is undersaturated with respect to calcite and supersaturated in respect to dolomite. Dolomitization can occur in a brakish water zone resulting from freshwater and sea water (Badioazamati, 1973). The ions of Mg^{+2} are supplied by the marine water and the undersaturation of $CaCO_3$ occurs with the mixing of the two waters. Holland (1964) and Mathews (1971) concluded that when two $CaCO_3$ saturated waters are mixed they become undersaturated with respect to calcite. The Dorag Dolomitization Model is used for the dolomitization by mixture of sea and freshwater (Badiozamati, 1973) (Fig. 1.7). Hardie (1987) discussed weaknesses in the mixing zone model produced by Badiozamati as follows: 1) the range of freshwater seawater mixture is small in disordered dolomites; 2) lack of evidence of dolomitization taking place in the mixing zone environments; 3) the trace elements in dolomites do not show the dolomitization in fluids and; 4) isotopic fractionation is used to support a problem that is not resolved (Land 1971). Isotopic data by Ramírez (2000) in the dolomites of the Lares Limestones and the Montebello Member of the Cibao Formation suggest dolomitization in a mixing zone environment.
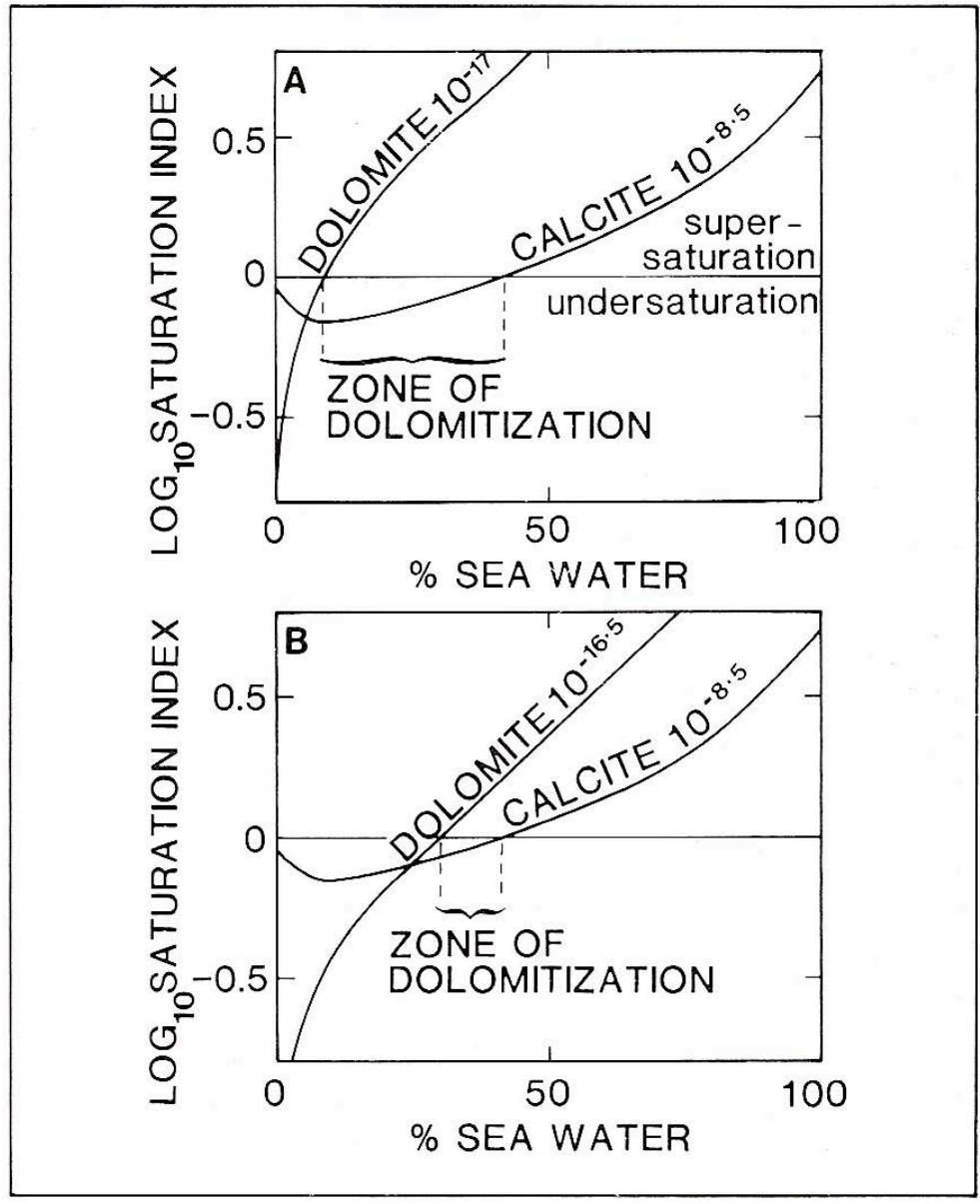
Figure 1.7: Theorical saturation relations of dolomite and calcite in
mixtures of seawater and meteoric water at 25°C (Hardie, 1986).

1.5 Stable Isotopes

Stable isotopes can be used to determine the temperature during crystallization and the composition of the fluid. This investigation will use isotopes analysis to have an idea of the environment were dolomites were precipitated; mixing zone, seawater, freshwater or meteoric environments. The values of stable isotope were plotted using the Lohmann's graph (1982) (Fig. 1.8). The range values between 0 to 4.00 $\&^{18}O$ and from 0 to 2 $\&^{13}C$ indicated marine zone. The values 1 to $3^{18}O$ and from 0 to -8 $\&$ ^{13}C indicated mixing zone. The values -2 to -4 $\&^{18}O$ and from -4 to -8 $\&^{13}C$ indicated meteoric zone.
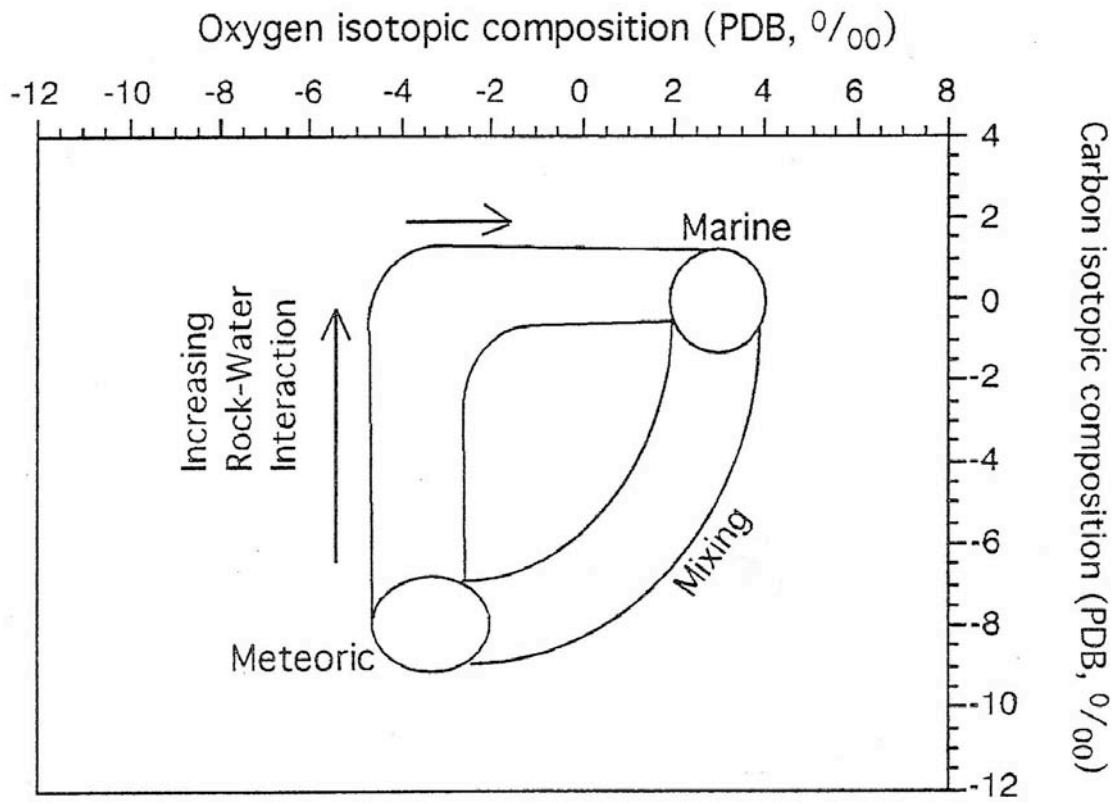
Figure 1.8 Lohman's (1982, 1988) interpretation of shifts in carbon and oxygen isotopic compositions during meteoric and meteoric-marine diagenesis.

Chapter 2

2.1 Fluid Inclusions Analysis

2.1.1 Introduction

Fluid inclusion analyses were done for the first time in 1792 by Dolomieu. He was the first to report inclusions in quartz filled with petroleum (Goldstein and Reynolds 1994). Fluid inclusions have been used during the last ten years by many investigators in sedimentary rocks. Fluid inclusions are fluid filled vacuoles found in minerals. The fluids are enclosed within a crystal of amorphous solids. These fluids may have the fluid of ancient diagenetic environments, with proxies for the temperatures and pressures present during the formation of the mineral. The technique provides detailed information on the thermal history and temperature of sedimentary rocks. There are four possibilities for the origin of fluid inclusions: primary, secondary, pseudosecondary, and unknown (Goldstein and Reynolds, 1994).

The primary inclusion results when any process interfere with the growth of a crystal. Some cracks occurred in a crystal and these imperfections result in a subsequent irregular growth of the crystals and trapping the inclusion in the new imperfectly grown crystals (Roedder 1984) (Fig. 2.1). In dolomites the primary inclusions occur in a definite growth zonation. The most common fluids inclusions in dolomites are cloudy and rhombohedra.

Secondary inclusions are produced after a crystal growth is completed. If crystals are fractured in the presence of fluid with a finite solubility, the fluids enter in the fracture and dissolve and recrystallized the host crystal. If the process of dissolution continues and the amount of a new crystal surfaces is reduced, a new secondary inclusions results and it is denominated necking down (Roedder, 1984) (Fig.2.2). Necking down is a post-entrapment in

which large, irregular inclusions move more towards morphological equilibrium splitting into several smaller, more equant inclusions (Fig. 2.2).

There are different variables that affect necking down; temperature, fluid and mineral composition, original size and shape, and the time of the fluid inclusions. The process of the necking down involves the dissolution-reprecipitation and dissolution of the fluids. A long time is usually needed for a significant necking down to occur but some experiments show that necking down in soluble minerals at high temperatures occurs rapidly, (Pecher, 1981; Brantley et al., 1990, Brantley, 1992). Brantley (1992) suggested that the microcraks of quartz may heal within 100°C or less or as low as 200°C in the presence of dilute pore fluids. The size and the shape of the fluids inclusions may be affected by necking down. Primary inclusions are formed by the growth of zones. During the process of necking down fluids are trapped in different morphologies. The temperature present during necking down causes some irregularities in the shape of the fluids inclusions. The change in fluid composition is one of the control phenomena in necking down (Goldstein and Reynolds 1994).

The process of necking down affects the interpretation of the physical and chemical history of the fluid inclusions. Figure 2.3 shows the relationship between de P -T aqueous fluid inclusions in the subsurface. If the temperature is 25°C all of the liquids are trapped at surface conditions in one phase diagram (point A). If necking down occurs at this point (point B) then the fluids have the same density of the original inclusions (Goldstein and Reynolds 1994) (Fig. 2.3). Also, when cooling down occurs in point C, the neck down inclusions will have the same density of the original inclusions. If we continue cooling to point D they produce necking down in the fluid inclusions so inclusions have the same density of the original single fluid. The pseudosecondary inclusion is trapped after an early phase of host crystal growth. The process is

finished, typically within a healed fracture, before all crystal growth is completed. (Roedder 1984) (Fig. 2.4).
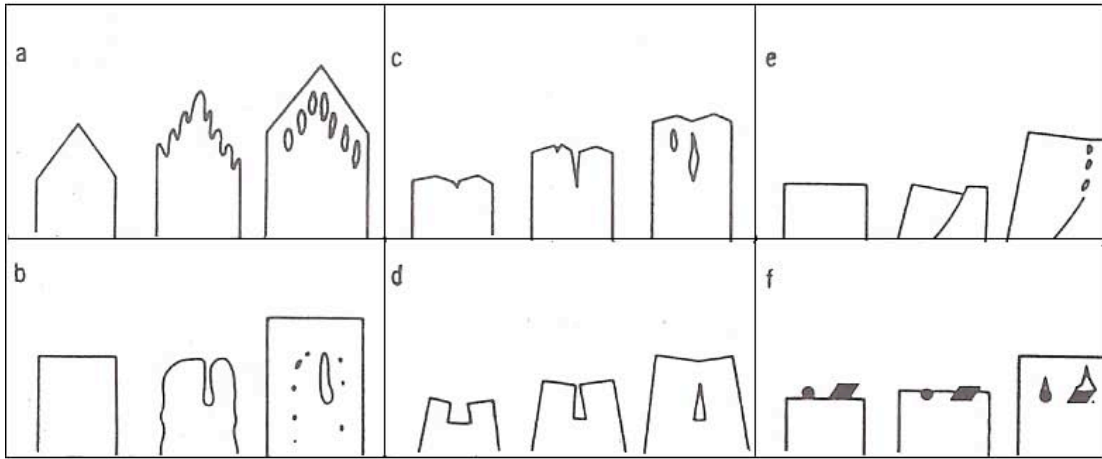
Figure 2.1: Mechanism for trapping a primary fluid inclusion (Roedder, 1984).
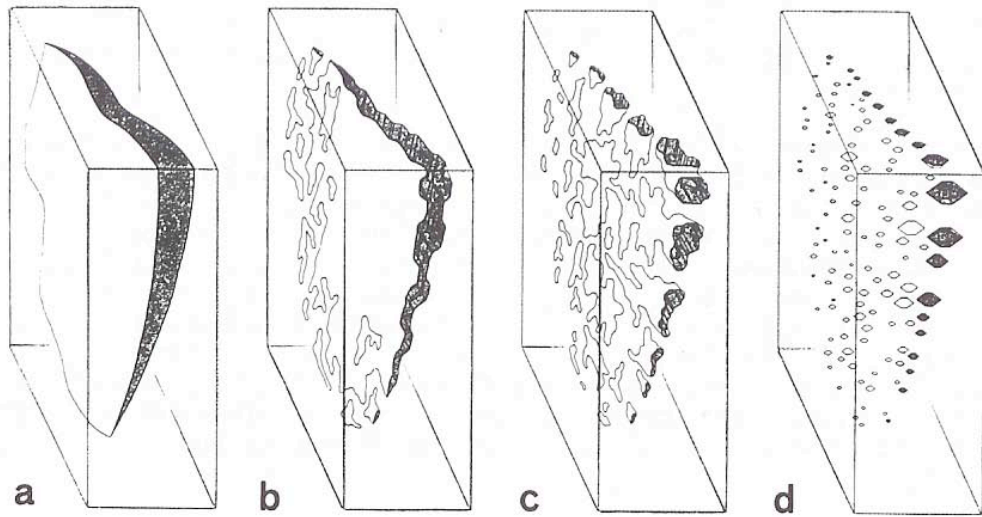
Figure 2.2: Stage in the healing or "necking down" of a crack in crystals quartz,resulting secondary inclusion (Roedder, 1984).
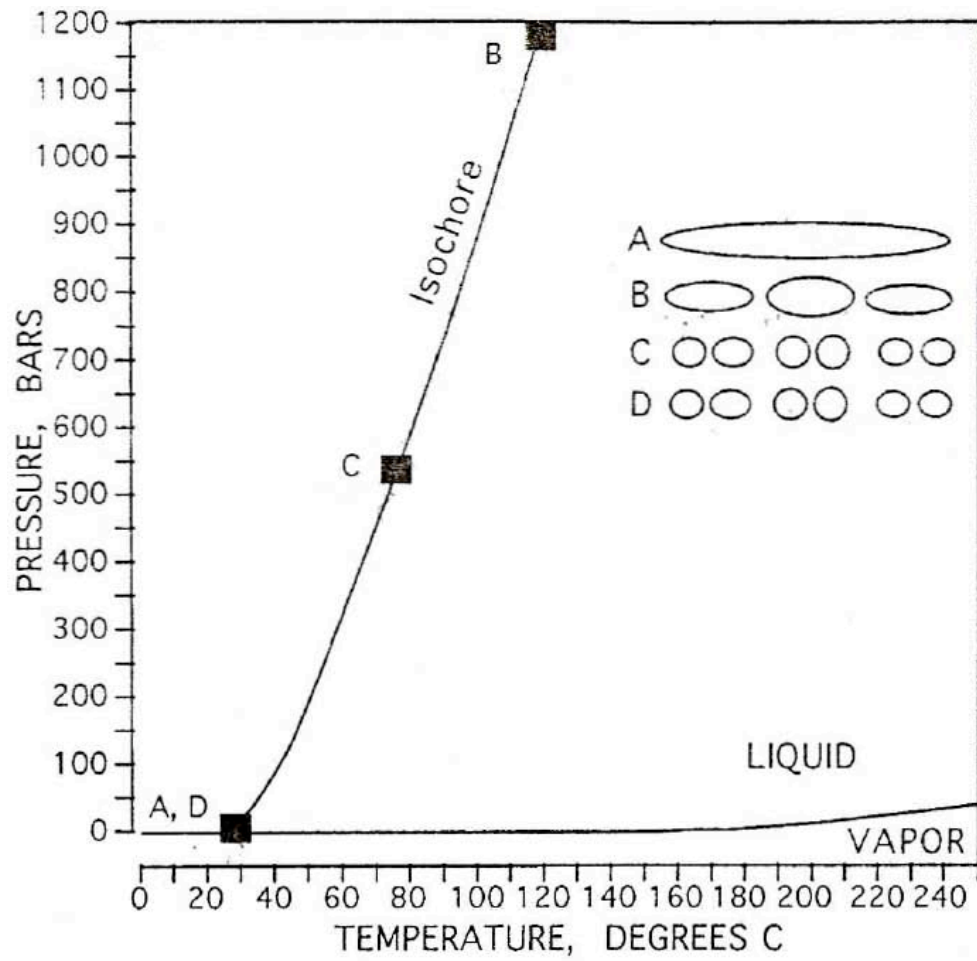
Figure 2.3 P-T phase diagrams for pure water (Goldstein and Reynolds, 1994).
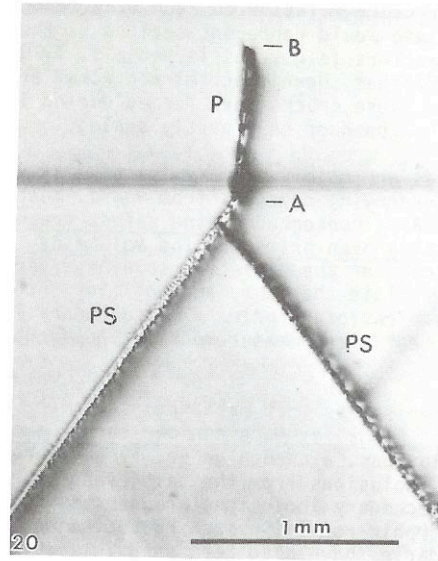
Figure 2.4: Photomicrograph of a pair of pseudosecondary inclusions in fluorite
(Roedder, 1984).

Fluid inclusions can be trapped during recrystallization of diagenetic minerals. Recrystallization involves a compositional change from somewhat unstable to a more stable mineral phase during a process of dissolution and reprecipitation. During the growth of the crystals contamination occurs with other crystals of similar or different minerals (Goldstein and Reynolds, 1994). This process of contamination of the crystal is denominated accidental. In dolomite, the recrystallization is detected by looking for rhombohedra with cloudy, inclusion-rich cores. At low temperatures recrystallization in diagenetic systems have a high solubility.

During the process of recrystallization of unstable precursor minerals the fluids in the mineral inclusion will re-equilibrate with the outside fluids because the inclusions will be opened. The inclusion cavities present during the process of recrystallization provide a record of the conditions of recrystallization rather than the original precipitation of the mineral.

To determine the thermal re-equilibration and temperature of the entrapment we consider inclusions that were trapped at the same time (consistent data). These fluid inclusions should have the same homogenization temperature, the same compositional data, and should suggest similar diagenetic environments (Goldstein and Reynolds, 1994). These groups of co-genetic fluid inclusions that occupy an individual petrographic feature are denominated Fluid Inclusions Assemblages (FIA). Since they provide detailed information about the fluid history, FIA, is the best method to be applied in sedimentary rocks. FIA are trapped at the same geologic time by a process in which the fluid inclusions are enclosed in a host mineral.

The diagenetic environment of fluid inclusions entrapment is determined using microthermomety (Goldstein and Reynolds 1994). This is a technique that measures the temperature of thermally-induced fluid inclusions by observing them under the microscope at high magnification. This technique documents the homogenization temperature at which

minerals are formed and the salinity of the trapped fluids. The homogenization temperature (Th)

is the temperature at which fluid inclusion is transform from multiple-phases (heterogeneous) to

one phase (homogeneous). This temperature is the minimum estimate of inclusions entrapment

temperature. The temperature of the entrapment indicates the original temperatures at with the

fluids inclusions were entrapped in the dolomites. To use the microthermomety technique the

samples cannot be previously overheated or cooled. One of the important parameters that will be

measured is the final melting temperature of ice (Tm). This temperature is important for

determining the salinity of aqueous fluid inclusions. To determine this temperature the samples

are prepared by freezing them. Vapor bubbles generated in the samples are used for the

interpretation of the phase equilibrium at low temperatures. Creating vapor bubbles in fluid

inclusions is important in order to develop phase diagrams. To determine the eutectic

temperature (Te) the fluid inclusions are frozen. The temperature of undercool of the fluid

inclusions, before it will freezes, is called the homogeneous nucleation temperature (Goldstein

and Reynolds, 1994). During the process of freezing the vapor bubbles disappear because they

have a lower density than liquid water, so the ice occupies all the spaces in the vacuum. This

causes the bubbles to shrunk. Vapor bubbles are produced to obtain the final melting

temperature and the eutectic temperature.

Heterogeneous entrapment is a process that involves one single-phase (liquid of vapor).

Single component water is calculated by four factors; pressure (P), volume (V), temperature (T)

and composition (X) (Fig. 2.5). Two thermodynamic gradients (P-T conditions) occur in

diagenetic systems (Fig. 2.5). The pressure gradient and an abnormal geothermal gradient of

10°C/km as well as the hydrothermal gradient 35°C/km are used to illustrate natural pore fluids

systems in a diagenetic realm (Fig. 2.5). Aqueous pore fluids exist in one-phase-liquid stability

field. The precipitation of diagenetic minerals occurs under these conditions; when the hydrostatic thermobaric gradient is at 35°C/km, the temperature is in 197°C/km and the pressure is 475 bars (point A) (Fig. 2.5). At these conditions the mineral do not grow perfectly and some of the pore fluids caused some imperfections in the crystal. At point C the temperature starts to cool. At this point the line of vapor-liquid is intersected and creates a minuscule vapor bubble that is formed in the inclusion (Fig. 2.5) (Goldstein and Reynolds, 1994). A natural path of P, V, and T will be created in the laboratory by the process of cooling and heating (Point F-E-D-C). The bubbles will be disappearing from point F to C. At point C the bubbles disappear because the inclusions become a single homogeneous liquid phase.

The temperature at point C is the homogenization temperature (Th) and it is the lower temperature obtained in the laboratory and characterized by bubble disappearance (Fig. 2.5) (Goldstein and Reynolds, 1994). This temperature is important in microthermomety of fluid inclusions because it provides an estimate temperature of entrapment of the fluid inclusion.
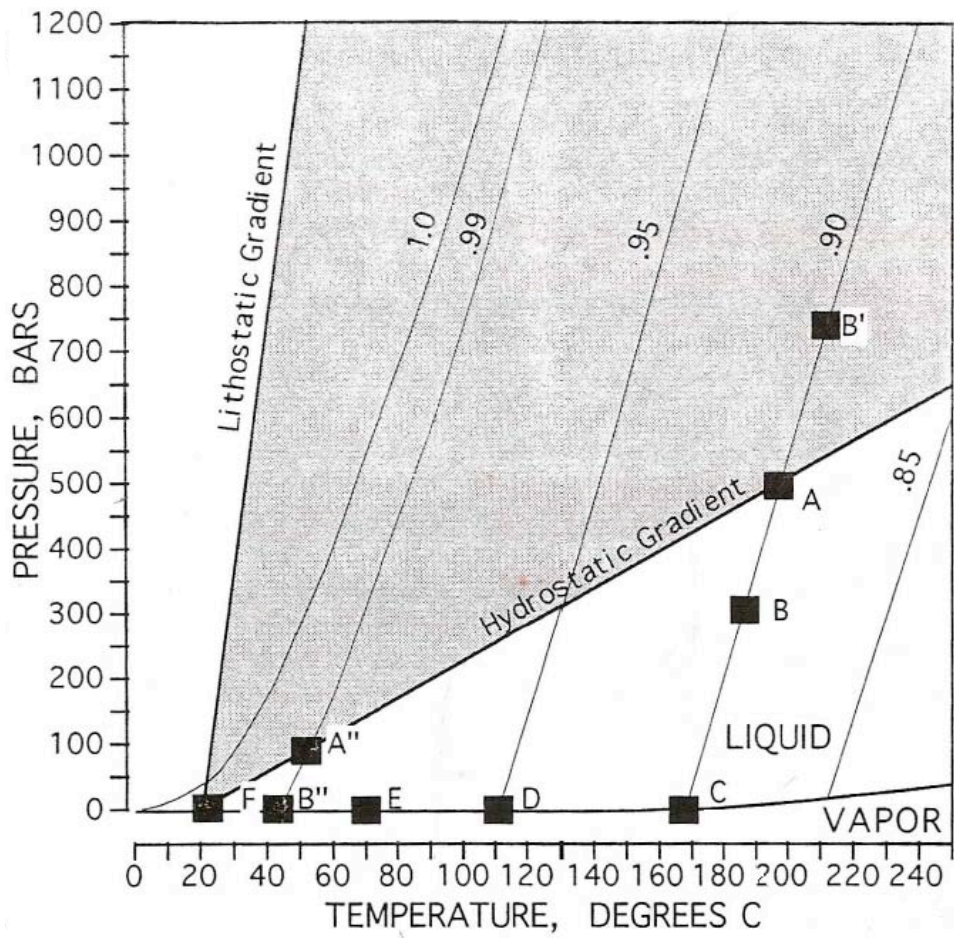
Figure 2.5.: P-T projection of the H_2O system for diagenetic P-T conditions (Goldstein and Reynolds, 1994).

There are different types of fluid inclusions; freshwater, H_2O-NaCl, Seawater, H_2O--NaCl-CaCl and H_2O--NaCl-CH4. A freshwater body is a body of water (pond, river, lake or stream) that contain less than <0.5 parts per thousand of salt. A freshwater system can be identified using microthermomety by the process of cooling and heating the inclusions. The melting temperature of ice for freshwater is 0°C (Goldstein and Reynolds, 1994). The freezing point of the seawater was calibrated form 0-60 ppt and Tm is from 0 to -3.1°C (Fig. 2.6). The equation to determine the salt concentrations in seawater in parts per thousands is;

$$\text{ppt seawater} = -0.1 \pm 19.22\theta - 0.93\theta \pm 0.34\theta \pm 0.34\theta 3$$

(θ is the depressed of freezing point in °C).

ppt seawater = -0.17 - 19.22Tm ice
- 0.93Tm ice^2 - 0.34Tm ice^3
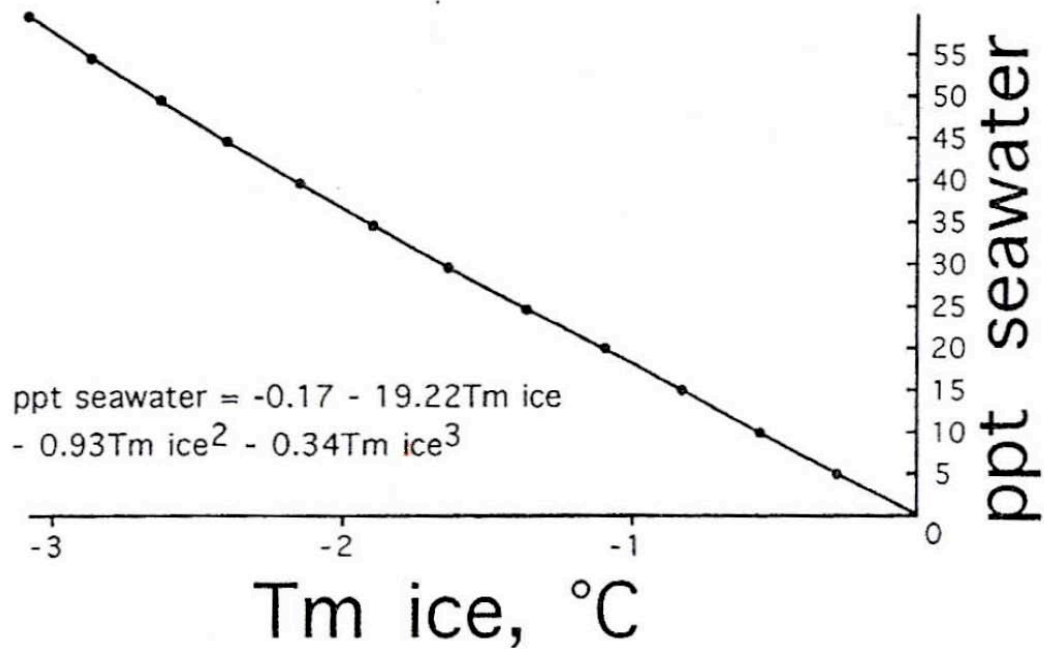
Figure 2.6: Seawater freezing point depression constructed by Lyaman and Fleming (1940) (Lyman and Fleming, 1940)

Metastability occurs if the bubble does not appear at the expected temperature and appears at a different interval of temperature. This process can be observed in a one-phase diagram that shows vapor or gas bubbles. When the temperature is at 100 °C (point A) and the inclusion is cooled, the bubble does not appear. If the fluids are cooled several tens of a degree this causes a spherical bubble in the fluid inclusion, returning to the equilibrium conditions of liquid-vapor curve (point C) (Fig. 2.7) (Goldstein and Reynolds, 1994).
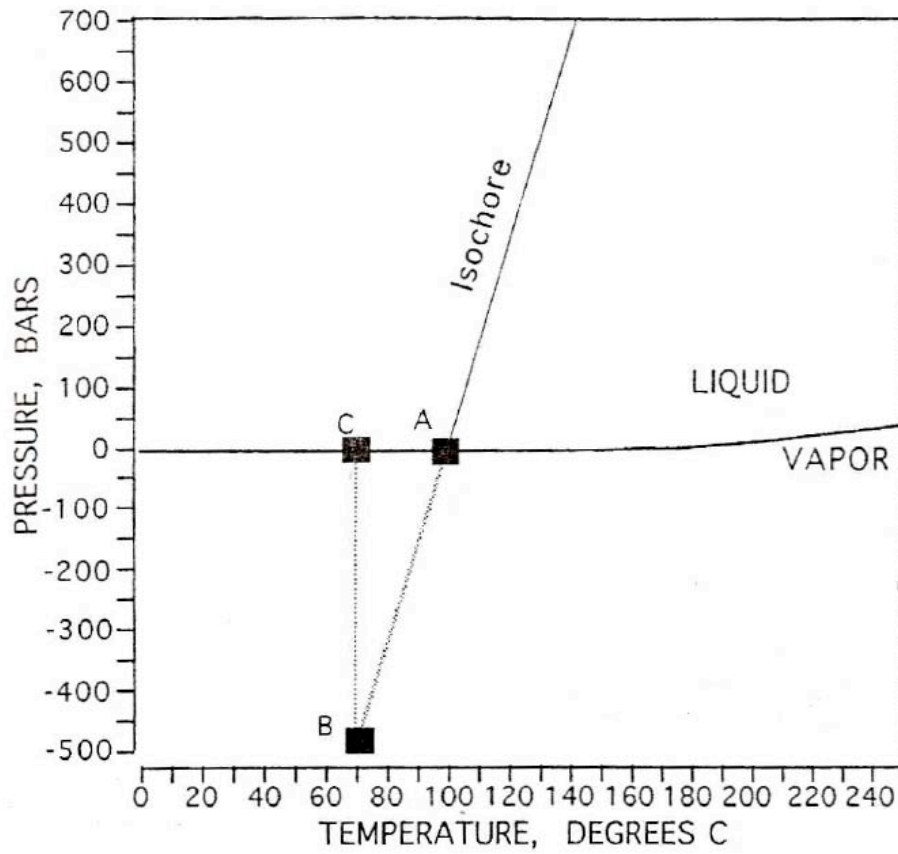
Figure 2.7: P-T phase diagram for pure water illustrating the amount of under-cooling typically required for nucleation of a vapor bubble (Goldstein and Reynolds, 1994).

2.2.2 Previous Work

Guzzy-Arredonde,. et al. (2007) worked in fluid inclusions of high temperature dolomites in the Lower Cretaceous Cupido Formation in Bustamante Canyon Mexico, northeast Mexico (Figure 2.8). They did petrography, strontium isotopes, major and minor trace elements, oxygen and carbon stable isotopes and fluid inclusion microthermomety. The Cupido Formation is part of the extensive carbonate platform from the northeastern Mexico to west Florida (Guzzy et al., 2007). This formation includes inner platform, platform margin and open marine facies. These carbonates represent a large system-scale of a prograding carbonate platform with a lower hierarchy of trangressive-regressive cycles that were developed during the late Hauterivian to early Aptian time (Guzzy et al., 2007). Stratigraphic sections measured in the Cupido Formation include inner platform, platform margin and outer platform facies that are dolomitic. There are two main geometries in the dolomites of this zone, (1) very irregular dolomite bodies and (2) tabular/ horizontal dolomite bodies. The irregular dolomites occur in the lower part of the Cupido Formation, where carbonate mud mounds are abundant. The rocks are partially dolomitic. Horizontal and tabular bodies of dolomite occur at the upper part of the Cupido Formation they consist of lime mud-poor, cyclic inner platform facies.

Two different types of dolomites are distinguished in the Cupido Formation. The types of dolomites most abundant are the replacement dolomite. Dolomite cements are also present. The crystals of the dolomite are very fine and contain peleoids and calcite cement veins. It is coarse to medium grained and contains skeletal grains and intraclasts (Guzzy et al., 2007).

The petrography analysis included one hundred thin sections. Depositional textures, grain constituents and cements were described. The fluid inclusions of the Cupido Formation are composed of two phases (liquid-vapor) and the shapes are rectangular to irregular. The homogenization temperature of the Cupido Formation Dolomite fluid inclusions dolomitic calcite suggests that these dolomites formed at high temperatures (range from 205° C to 217 ° C).

The petrography, cathodoluminescense, traces elements, oxygen isotopes and fluid inclusions microthermomety indicate that Cupido Formation dolomites were formed in a deep-burial diagenetic environment. The timing of dolomitization is unknown for the Cupido Formation but the geologic history suggest that dolomitization probably occured during Late Cretaceous time at the Laramide Orogeny (Goldstein and Reynolds, 1994).

The Hogoton embayment is located in the northwestern shelf of the Anadarko Basin and embraces part of the southwestern Kansas, southeastern Colorado, the Texas panhandle, and the Oklahoma panhandle. Siemer and Ahr (1990) presented two diagenetic processes to explain the dolomitization of the Chase Group. First, an initial brownish, inclusion rich- dolomite that represent the sequence of the upper Chase Group formed by exposure to influx of brines which resulted by evaporitic conditions during cyclical low-stands of sea level. They suggested two events of "leaching" and then compaction.
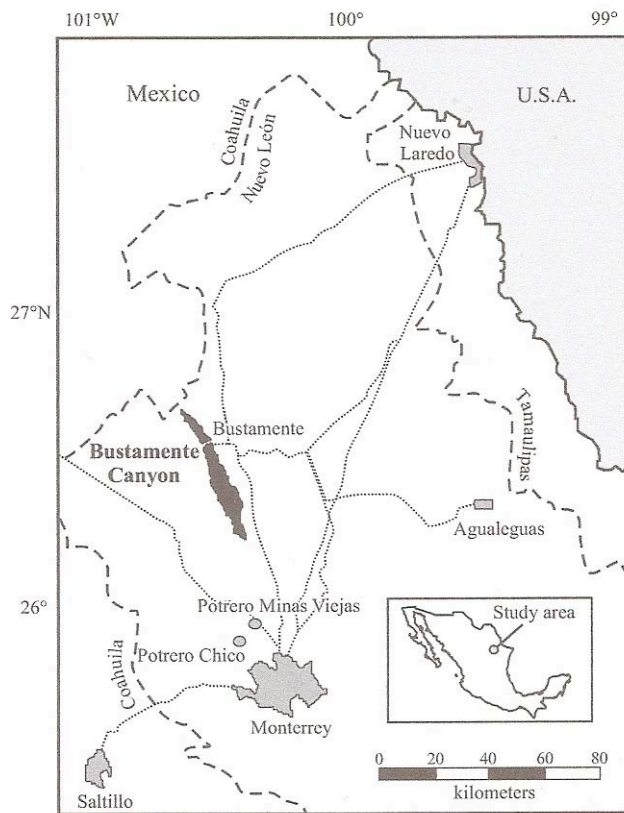
Figure 2.8: Location map of the Bustamante Canyon, State
of Nuevo Leon, Mexico (Guzzy-Arredondo et al., 2007).

Petrography shows that the lower Krider Member is an oncolitic, sucrosic dolostone with anhydrite, massive replacement of quartz, pyrite, phosphates, minor organic matter, chert and quartz silt. Cathodoluminescense (CL) analysis showed dolomitization by replacement with cementation dominant. The fluid inclusion analysis indicated that the dolomites of the lower Krider Member are aqueous one phase inclusions. Most of the fluid inclusions in the Chase Group Carbonates are aqueous and are composed of two phases. The U-Pb isotopic data indicate that uranium in the dolomite of the lower Krider Member was not sydepositional. The analysis of fluid inclusions, U-Pb and stratigraphic relationships suggest that during the Permian a reflux of low-temperature, Mg bearing brines precipitated the U-bearing dolomites and replaced earlier dolomites in the lower Krider Members and others members of the Chase Group (Guzzy et al., 2007).

Chapter 3

Methodology

This chapter includes details about the methodology use in this research. The laboratory work includes the process of making thin sections and the microthermometric fluid inclusions analysis.

3.1 Terminology

a. Homogenization temperature (Th) - is the temperature at which fluid inclusions is transform from multiple-phases (heterogeneous) to one phase (homogeneous). It is the temperature at which the minerals are formed and the fluids inclusions are trapped. This temperature is the minimum estimate of inclusions entrapment temperature.

b. Final melting temperature of ice (Tm) - this temperature is used to interpret the salinity of the rocks.

c. Shrunk- where the ice melts and the bubbles are composed of water vapor.

d. Jerk- the process where water turns into ice creating bubbles in the inclusions walls and causing deformations.

e. Alteration- is the changes of the chemical or mineralogical composition of the rocks that occurred due to weathering or hydrothermal solutions.

f. Dolomitization- is the process that limestone is partially converted to dolomite rock by a replacement of the original composition of calcite by magnesium carbonate.

3.2 Laboratory Work

3.2.1 Methodology to make thin sections for fluid inclusions

This investigation used fluid inclusion techniques developed by Goldstein (1994). This methodlogy is as follows:

1) Samples of dolomite from the core NC5, IAS-4, Garrochales, NC-9, NC-10, IAS- and NC-6, located along the Puerto Rico north coast, were used mainly because they have been studied in detail (petrography, XRD, strontium isotopes, stable isotopes, and elemental concentrations) by Ramírez (2000).

2) Thirty thin sections were prepared at the Geology Department Thin Sections Laboratory University of Puerto Rico at Mayagüez. The sections were prepared following the procedures specified for the fluid inclusion analysis described below:

   a. Impregnation techniques that involve heat and high pressure were avoided.

   b. Samples were cut gently. Coolant was used when a high speed trim saw was use.

   c. There are three different thick plates that can be used to prepare the thin sections: quick plate, double polished plate and cleavage fragments. In this study double polished plate will be used. Both faces of the samples must be polished to 5 microns.

   d. To obtain fluid inclusions, the dolomites evaluation and temperature monitoring processes were completed in the University ok Kansas.

3.2.2 Methodology to study fluid inclusions:

The petrographic analysis was focused on observations and descriptions of the minerals and rocks. The fluid inclusion microscope is similar to a standard microscope. However the transmitted light of the petrographic microscope have a long working distance objectives and a long working distance condenser to focus the sample within the stage and to focus the converging beam light into the sample. These petrographic microscopes provide the temperature and pressure conditions for the precipitation of minerals (Goldstein and Reynolds, 1994) (Fig. 3.1). The microscope has a trinocular mount with a closed circuit television (CCTV) or photography system mounted. Steps to measured fluid inclusions:

1. Fluid inclusions are small liquid bubbles that are trapped within the crystals. For the fluid inclusion analysis the internal parts of the minerals must be observed. In the microscope the internal and the external structures of the dolomites must be studied and the fluid inclusions present in the inner parts of the dolomites were analyzed.

2. In order to observe the fluid inclusions in the dolomites, the rock has to be divided into fragments. This process consists of submerging the thin sections in acetone during 5-6 hours. This dissolves the glue from the thin sections (Fig. 3.2). After dissolving the glue from the thin sections we can obtain the fragments of the rocks and observe the fluid inclusions in the dolomite fragments.

Figure 3.1: Petrographic microscope designed to observe fluid inclusions
(University of Kansas).
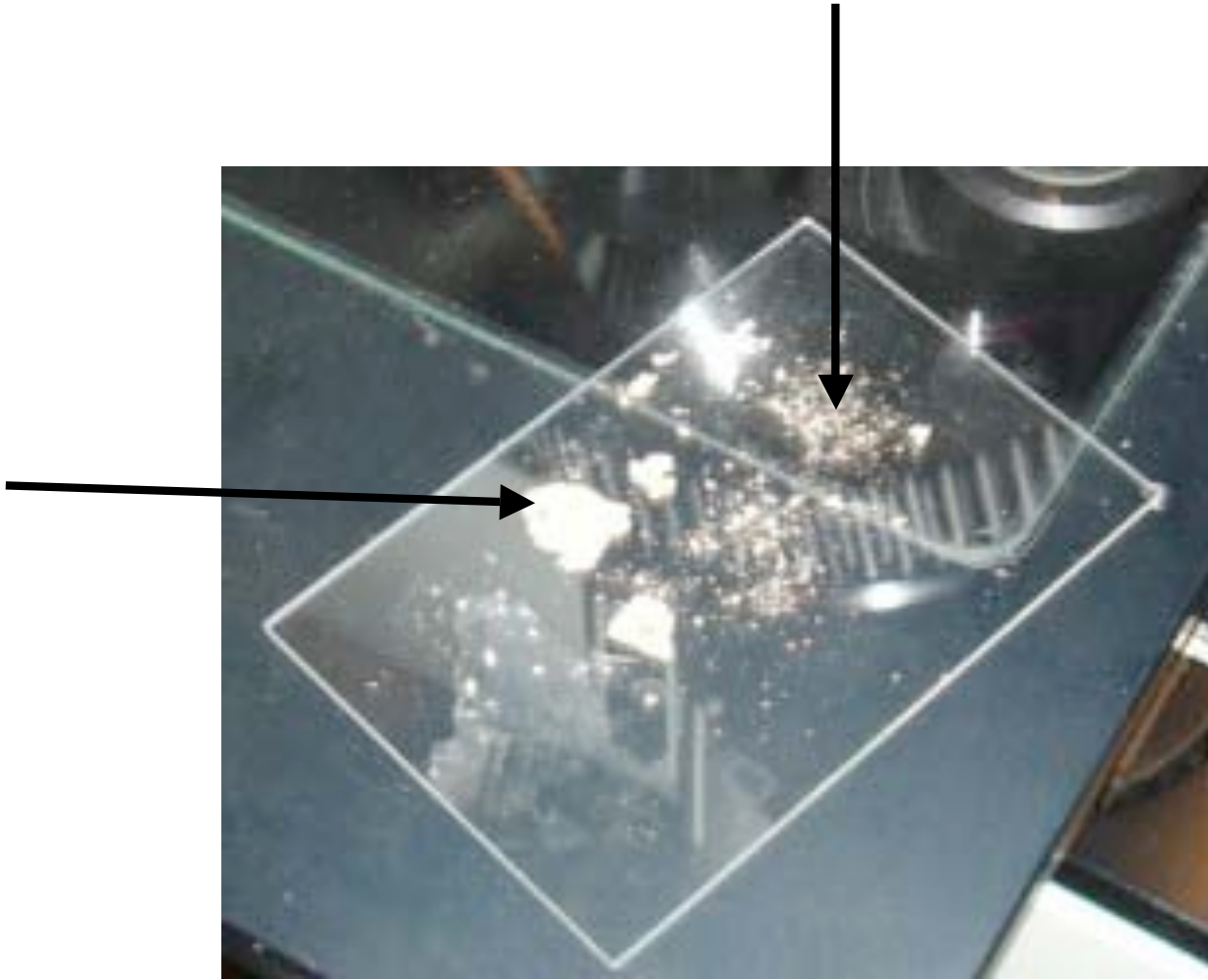
Figure 3.2: Fragments of dolomite obtained from the thin sections that have been removed by submerging the samples in acetone.

3. These fragments are analyzed using the microscope (Fig. 3.1). The fluid inclusions found in the dolomites were mapped and photographed (Fig. 3.3).
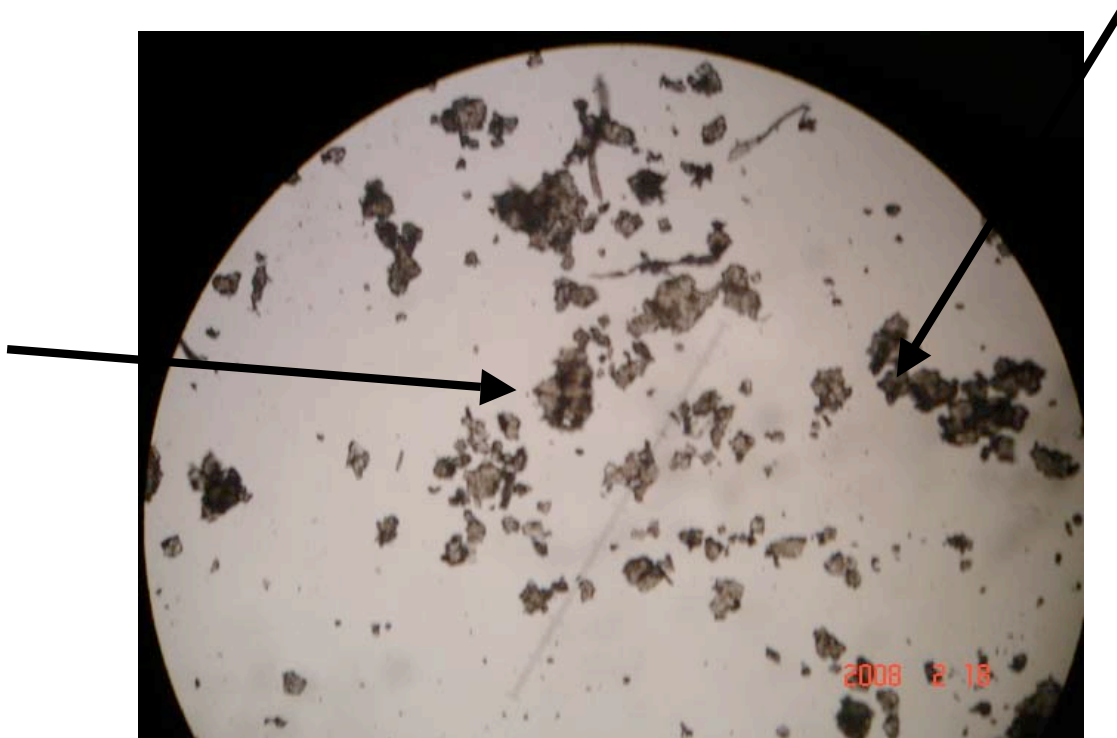
Figure 3.3: Examples of image used to map the dolomite crystals. The image shows the best crystals that are evaluated to measure the fluid inclusions.

4. The inclusions were then subjected to heating and cooling to observe changes. To produce the bubbles in the fluid inclusion analysis the fragments were heated. This process of heating increased the size of the bubbles. The samples of dolomites that contain the best fluid inclusions were raised to 125°C during 8 to 10 hours (Fig. 3.4). These samples were refrigerated 5 to 6 hours in a freezer. This process of heating and cooling caused the expansion of the bubbles. Photos of the changes were taken in the inclusions to detected bubbles that can be measure.

5. If the bubbles are present we can measure the fluids by subjecting them to cooling and heating. Liquid nitrogen will be used to cool the samples (Fig. 3.5). Temperature measurements were done using the Linksys software.

Figure 3.4: Equipment to heat the samples at temperature of 125° Cand175°C
available at the University of Kansas.

Figure 3.5: Equipment used to measure homogenization temperature of fluid inclusions in dolomites available at the University of Kansas.

6. To measure the homogenization temperature in fluid inclusions, the process of cycling was used (Fig. 3.6). When ice melts in the inclusion the bubble increase in size because the liquid H_2O occupies less volume than ice. The process of shrinkage indicates the growing of the ice in the bubbles. The absence or presence of ice is called cycling and it is an effective method to determine the Tm ice in the fluid inclusions. The process of cycling is described below:

    a. Cooling of the inclusions by freezing the bubbles (nucleation temperatures). The inclusions must be heated rapidly while observing for changes in size of the vapor bubble (Goldstein and Reynolds, 1994).

    b. If the bubble reappears the approximated position of the Tm ice can be recorded. If there are not any changes in the bubble, the samples were heated until 0°C to make sure the ice melted. They were freezed again to supercool the nucleation temperature (step a).

    c. The inclusions were heated just above the Tm (step b) and then were cooled again to the nucleation temperature. The temperature at which the bubbles appeared was recorded again for a second time.

    d. If the bubbles do not jerk in the inclusions the temperature was raised until the temperature in step c. The inclusions were then heated to higher temperatures and then the process was repeated again until they show the nucleation temperature. If the bubbles do not appear, the process was repeated many times until the jerk is seen.

    e. If the bubbles were jerked this indicated that ice melted totally (step c) and the temperature of homogenization was measured.
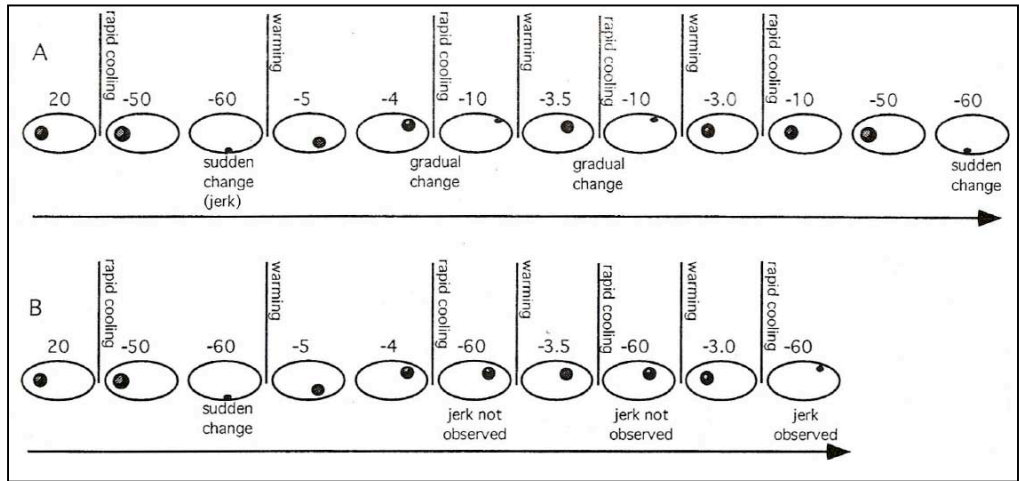
Figure 3.6: Schematic representation of the cycling process used to determine Tm ice for small inclusions prevalent in diagenetic minerals (Goldstein and Reynolds, 1994).

7. The final melting temperature of ice (Tm ice) is used to estimate the bulk salinity of the fluid inclusions. The salinity in the fluids indicates if the inclusions retained fresh water or marine water. (Goldstein and Reynolds, 1994). Salinity estimates were done with the Tm ice using the calibrations proposed by Potter and others (1978). The equation proposed by Hall and others (1988), Bodnar (1992a, b) provided the salinity of the fluids. The equation is expressed as: Salinity (wt. %) $=0.00+1.78\theta-0.0442 \theta^2+0.000557 \theta^3$; where θ is the depression of freezing point (magnitude Tm ice is depressed below 0.0° C) (Table 3.1).

FPD	.0	.1	.2	.3	.4	.5	.6	.7	.8	.9
0.	0.00	0.18	0.35	0.53	0.71	0.88	1.05	1.23	1.40	1.57
1.	1.74	1.91	2.07	2.24	2.41	2.57	2.74	2.90	3.06	3.23
2.	3.39	3.55	3.71	3.87	4.03	4.18	4.34	4.49	4.65	4.80
3.	4.96	5.11	5.26	5.41	5.56	5.71	5.86	6.01	6.16	6.30
4.	6.45	6.59	6.74	6.88	7.02	7.17	7.31	7.45	7.59	7.73
5.	7.86	8.00	8.14	8.28	8.41	8.55	8.68	8.81	8.95	9.08
6.	9.21	9.34	9.47	9.60	9.73	9.86	9.98	10.11	10.24	10.36
7.	10.49	10.61	10.73	10.86	10.98	11.10	11.22	11.34	11.46	11.58
8.	11.70	11.81	11.93	12.05	12.16	12.28	12.39	12.51	12.62	12.73
9.	12.85	12.96	13.07	13.18	13.29	13.40	13.51	13.62	13.72	13.83
10.	13.94	14.04	14.15	14.25	14.36	14.46	14.57	14.67	14.77	14.87
11.	14.97	15.07	15.17	15.27	15.37	15.47	15.57	15.67	15.76	15.86
12.	15.96	16.05	16.15	16.24	16.34	16.43	16.53	16.62	16.71	16.80
13.	16.89	16.99	17.08	17.17	17.26	17.34	17.43	17.52	17.61	17.70
14.	17.79	17.87	17.96	18.04	18.13	18.22	18.30	18.38	18.47	18.55
15.	18.63	18.72	18.80	18.88	18.96	19.05	19.13	19.21	19.29	19.37
16.	19.45	19.53	19.60	19.68	19.76	19.84	19.92	19.99	20.07	20.15
17.	20.22	20.30	20.37	20.45	20.52	20.60	20.67	20.75	20.82	20.89
18.	20.97	21.04	21.11	21.19	21.26	21.33	21.40	21.47	21.54	21.61
19.	21.68	21.75	21.82	21.89	21.96	22.03	22.10	22.17	22.24	22.31
20.	22.38	22.44	22.51	22.58	22.65	22.71	22.78	22.85	22.91	22.98
21.	23.05	23.11	23.18							

Table 3.1: Table of salinities (wt. % NaCl) that correspond to freezing point depression for fluid inclusions in the presence of a vapor bubble (Bodnar, 1992). FDP is absolute value of Tm ice ºC; after Bodnar (1992).

3.3 Isotopes Methodology

Stable isotopes in the dolomites were analyzed by macrospectometry at the University of Kansas. The samples analyzed are from cores of the north coast of Puerto Rico including; Garrochales, IAS-1, IAS-4, and NC-5. Samples from these cores were analyzed by fluid inclusions analysis. Approximately 69 samples were processed. Samples were selected only if they had 100 percent dolomites. Samples with calcite and foraminifers were also analyzed for comparisons. The Thermo Finnigan MAT 253 Dual Inlet System was used with acid carbonate phosphate to burn the samples so it produces gas analyzed by pure CO_2 to be used in the mass spectrometer (Fig. 3.7).

Figure 3.7: Microscope used to drill hand sample to obtain the samples of dolomites. Available at the University of Kansas.

Chapter 4

Results

4.1 Fluid Inclusions

In this study thirty (30) thin sections were analyzed for fluid inclusions. Not all the thin sections had adequate fluid inclusions (Fig. 4.1) after analized. Most of the fluid inclusions present in the dolomites were empty. The process of preparing thin sections may have destroyed the fluid inclusions in the dolomites (Fig. 4.2). Weathering may also damage the fluid inclusions. If the samples of dolomite are polished more than required it may also destroy the fluid inclusions.
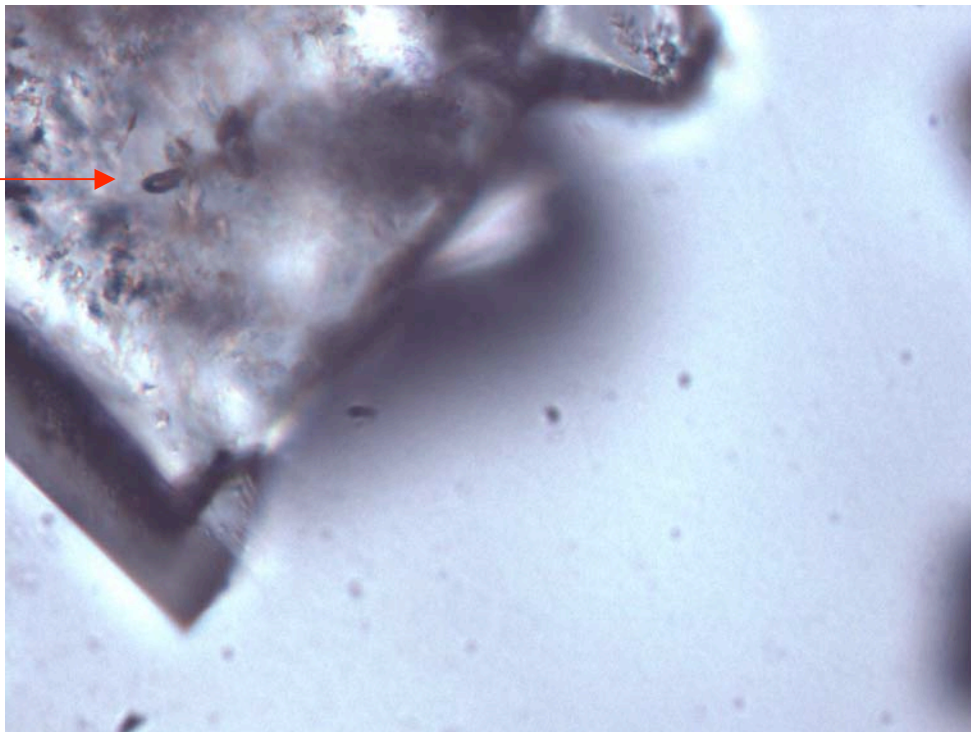
Figure 4.1: Empty fluid inclusions in dolomite may have occurred due to weathering and/or polishing too much the samples.
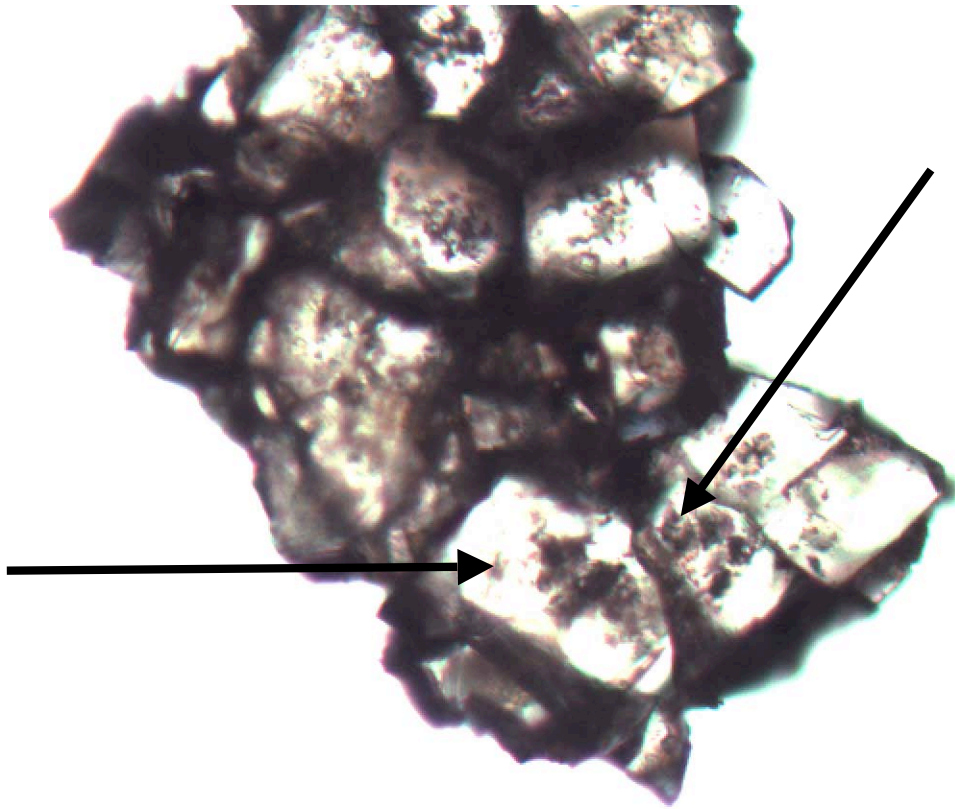
Figure 4.2: Dolomites with empty inclusions, consequence of polishing or
weathering. These empty spaces do not produce the bubbles
that need to be measured.

Using the equations proposed by Hall et al. (1988) and Bodnar (1992 a, b) we obtained the salinity of the fluid inclusions. The equation is expressed as:

$$\text{wt. (\%)} = 0.00 + 1.78\theta - 0.0442\,\theta^2 + 0.000557\,\theta^3;$$

where θ is the depression of freezing point (magnitude Tm ice is depressed below 0.0° C).

In the dolomite sample of IAS-4 (510.1m) the temperatures obtained were 0.0 and -0.1. The dolomite samples at IAS-4 (420.1m) produced a final melting temperature of 0.0 (Table 4.1). To validate the results, the procedures were repeated more than five times. The samples with the best fluid inclusions (best bubbles) are in Figures 4.3 and 4.4. The temperature obtained was substituted in the following equation:

$$\text{Wt. (\%)} = 0.00 + 1.78\theta - 0.0442\,\theta^2 + 0.000557\,\theta^3;$$

$$\text{Wt (\%)} = 0.00 + 1.78(0) - 0.0442(0)^2 + 0.000557\,(0)^3$$

$$\text{Wt (\%)} = 0.00$$

Table 4.1: This table show the values of fluid inclusions obtained in the samples of IAS-4 (510.1) and IAS-4 (420.1). These two cores have high percentages of dolomite and adequate fluid inclusions to measure.

Samples	Data obtained using fluid inlcusions
IAS-4 (510.1m)	0.00
	0.01
IAS-4 420.1m	0.00
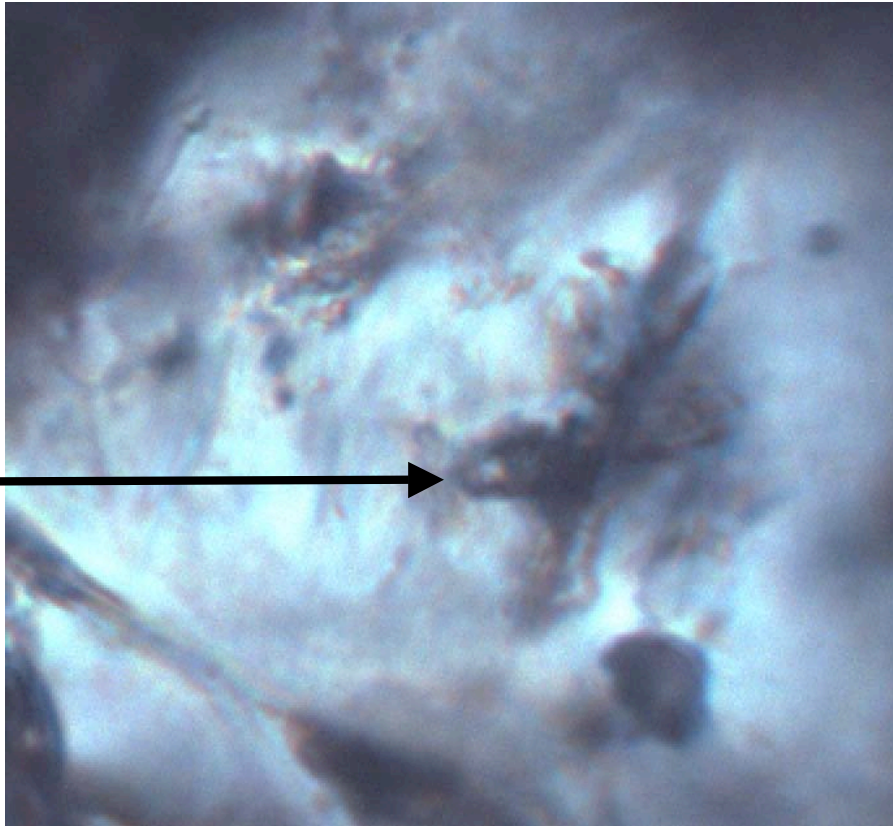
Figure 4.3: Sample of dolomite with fluid inclusions (IAS-4, 510.1m). In this microphotograph we can observe the fluid inclusions. These fluid inclusions created the bubbles that we measured to obtain the final melting temperature.
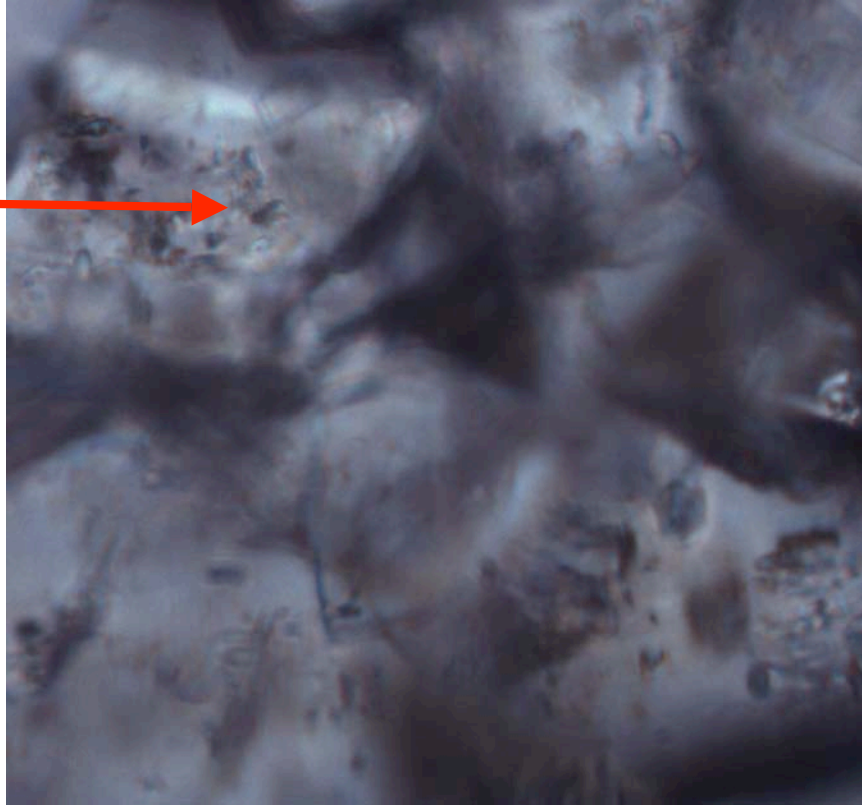
Figure 4.4: Sample of dolomite with fluid inclusions (IAS-4,510.1m). In this microphotograph we can observe the surface of the dolomite (lower part of the picture). In the upper part of the thin section (identify by a red arrow) we can observe the fluid inclusions that we measured to obtain the salinity.

The data obtained was plotted in Table 4.2 to show the environment were these fluid inclusions formed. According to the table, the salinity of freshwater is 0.00, the salinity in mixing zone is from 1.00 to 3.00 and the concentration of salinity in sea water is more than 3.00 wt % NaCl.

In the sample IAS-4 (510.1m) and IAS-4 (590.5m) the temperature obtained was 0.0 wt% NaCl (FDP) (Absolute value of Tm ice in °C after Bodnar (1992) and the percent of salinity from the equation is 0.0 wt%NaC). When these values are plotted in the table, they show the fluid inclusions in IAS-4 (510.1m), IAS-4 (590.5m) that are composed of freshwater.

Table 4.2: Table of salinities (wt. % NaCl) that correspond to freezing point depression for fluid inclusions in the presence of a vapor bubbles (Celsius) (Bodnar, 1992). FDP is absolute value of Tm ice ºC; after Bodnar (1992). The rectangular symbol ( ) indicates the zone of my results in Table 4.2.

FPD	.0	.1	.2	.3	.4	.5	.6	.7	.8	.9
0.	0.00	0.18	0.35	0.53	0.71	0.88	1.05	1.23	1.40	1.57
1.	1.74	1.91	2.07	2.24	2.41	2.57	2.74	2.90	3.06	3.23
2.	3.39	3.55	3.71	3.87	4.03	4.18	4.34	4.49	4.65	4.80
3.	4.96	5.11	5.26	5.41	5.56	5.71	5.86	6.01	6.16	6.30
4.	6.45	6.59	6.74	6.88	7.02	7.17	7.31	7.45	7.59	7.73
5.	7.86	8.00	8.14	8.28	8.41	8.55	8.68	8.81	8.95	9.08
6.	9.21	9.34	9.47	9.60	9.73	9.86	9.98	10.11	10.24	10.36
7.	10.49	10.61	10.73	10.86	10.98	11.10	11.22	11.34	11.46	11.58
8.	11.70	11.81	11.93	12.05	12.16	12.28	12.39	12.51	12.62	12.73
9.	12.85	12.96	13.07	13.18	13.29	13.40	13.51	13.62	13.72	13.83
10.	13.94	14.04	14.15	14.25	14.36	14.46	14.57	14.67	14.77	14.87
11.	14.97	15.07	15.17	15.27	15.37	15.47	15.57	15.67	15.76	15.86
12.	15.96	16.05	16.15	16.24	16.34	16.43	16.53	16.62	16.71	16.80
13.	16.89	16.99	17.08	17.17	17.26	17.34	17.43	17.52	17.61	17.70
14.	17.79	17.87	17.96	18.04	18.13	18.22	18.30	18.38	18.47	18.55
15.	18.63	18.72	18.80	18.88	18.96	19.05	19.13	19.21	19.29	19.37
16.	19.45	19.53	19.60	19.68	19.76	19.84	19.92	19.99	20.07	20.15
17.	20.22	20.30	20.37	20.45	20.52	20.60	20.67	20.75	20.82	20.89
18.	20.97	21.04	21.11	21.19	21.26	21.33	21.40	21.47	21.54	21.61
19.	21.68	21.75	21.82	21.89	21.96	22.03	22.10	22.17	22.24	22.31
20.	22.38	22.44	22.51	22.58	22.65	22.71	22.78	22.85	22.91	22.98
21.	23.05	23.11	23.18							

The fluid inclusions in the sample IAS-4 (510.1m) produced a final temperature of -.0.01. This value was substituted in the following equation:

$$Wt.\,(\%) = 0.00 + 1.78\theta - 0.0442\,\theta^2 + 0.000557\,\theta^3;$$

$$Wt.\,(\%) = 0.00 + 1.78(-0.01) - 0.0442(-0.01)^2 + 0.000557\,(-0.01)^3;$$

$$Wt.\,(\%) = -\,0.017$$

The data obtained was evaluated again using the graph of Bodnar (1992). This represents that the fluid inclusion is composed of freshwater (Table 4.3).

Table 4.3: Table of salinities (wt. % NaCl) that correspond to freezing point depression (Celsius) (Bodnar, 1992). FDP is absolute value of Tm ice °C; after Bodnar (1992). Note: The rectangular symbol (▭) indicates the zone of my results in the Table 4.3.

FPD	.0	.1	.2	.3	.4	.5	.6	.7	.8	.9
0.	0.00	0.18	0.35	0.53	0.71	0.88	1.05	1.23	1.40	1.57
1.	1.74	1.91	2.07	2.24	2.41	2.57	2.74	2.90	3.06	3.23
2.	3.39	3.55	3.71	3.87	4.03	4.18	4.34	4.49	4.65	4.80
3.	4.96	5.11	5.26	5.41	5.56	5.71	5.86	6.01	6.16	6.30
4.	6.45	6.59	6.74	6.88	7.02	7.17	7.31	7.45	7.59	7.73
5.	7.86	8.00	8.14	8.28	8.41	8.55	8.68	8.81	8.95	9.08
6.	9.21	9.34	9.47	9.60	9.73	9.86	9.98	10.11	10.24	10.36
7.	10.49	10.61	10.73	10.86	10.98	11.10	11.22	11.34	11.46	11.58
8.	11.70	11.81	11.93	12.05	12.16	12.28	12.39	12.51	12.62	12.73
9.	12.85	12.96	13.07	13.18	13.29	13.40	13.51	13.62	13.72	13.83
10.	13.94	14.04	14.15	14.25	14.36	14.46	14.57	14.67	14.77	14.87
11.	14.97	15.07	15.17	15.27	15.37	15.47	15.57	15.67	15.76	15.86
12.	15.96	16.05	16.15	16.24	16.34	16.43	16.53	16.62	16.71	16.80
13.	16.89	16.99	17.08	17.17	17.26	17.34	17.43	17.52	17.61	17.70
14.	17.79	17.87	17.96	18.04	18.13	18.22	18.30	18.38	18.47	18.55
15.	18.63	18.72	18.80	18.88	18.96	19.05	19.13	19.21	19.29	19.37
16.	19.45	19.53	19.60	19.68	19.76	19.84	19.92	19.99	20.07	20.15
17.	20.22	20.30	20.37	20.45	20.52	20.60	20.67	20.75	20.82	20.89
18.	20.97	21.04	21.11	21.19	21.26	21.33	21.40	21.47	21.54	21.61
19.	21.68	21.75	21.82	21.89	21.96	22.03	22.10	22.17	22.24	22.31
20.	22.38	22.44	22.51	22.58	22.65	22.71	22.78	22.85	22.91	22.98
21.	23.05	23.11	23.18							

4.2 Stable Isotopes

4.2.1 Stable isotopic analysis in Dolomites

Approximately 69 samples of dolomite were processed for stable isotopic analyses. The analyses were done in calcite and dolomites. The data of stable isotopes was used to determine if the dolomite show signs of alteration in meteoric, marine or mixed meteoric marine waters. The graph produced by Lohmann's (1982, 1988) was used to determine if the dolomites may have been altered in meteoric, mixing or marine environments (Fig. 1.3). The fluid inclusions analysis indicates that the dolomites could have been recrystallized in freshwater. Stable isotopic data support the possibility of recrystalization of the dolomite in freshwater.

Stable isotopic signatures in samples of IAS-4(590.5m) have marine water signatures (Fig. 4.5). Sample Garr (522.9m) have meteoric water signatures (Fig. 4.6). The stable isotopes of all samples range from -4.84 to -4.33 in $\delta^{18}O$ and from –7.20 to -6.67 in $\delta^{13}C$ (Table 4.4) (Appendix I). The stable isotopic signatures in the analysis of IAS-4 (420.1m) have marine water signatures (Fig. 4.7). The samples range in values form $\delta^{18}O$ 1.54 to 2.04 and $\delta^{13}C$ 0.72 to 1.19 (Table 4.4) (Appendix I). Analyses from NC-10 (454m) have meteoric water signatures (Fig. 4.8). The ranges of values of $\delta^{18}O$ are from -4.53 to -4.37 and $\delta^{13}C$ from -9.31 to -9.28 (Table 4.4) (Appendix I). All the isotopic values obtained from NC-10, Garr (522.9m), IAS-4 (420.1m), and IAS-1 (685.7m) were plotted in the graph of Lonhmann's (Fig. 4.5, Fig. 4.6 and Fig. 4.7).

Table 4.4: Values of stable isotopes of cores Garr (522.9m), IAS-4 (420.1m), and IAS-1 (685.7m). We obtained more than one value to corroborate if the dolomites had marine or meteoric isotopic signatures.

Samples	δ ^{13}C VPDB	δ ^{18}O VPDB
IAS-4 461.3m	1.40	1.68
	1.08	1.20
IAS-4 420.1m	1.19	1.54
	1.09	1.68
	0.72	2.02
	1.04	1.96
	0.95	1.95
	0.86	1.88
	1.06	1.73
	0.88	2.04
NC-10 (454m)	-9.31	-4.53
	-9.41	-4.37
	-9.28	-4.45
Garr (522.9)	-6.67	-4.59
	-7.20	4.84
	-6.72	-4.33
IAS-4 (590.5m)	0.57	1.32
	1.32	1.43
	1.22	1.33

Figure 4.5: Analysis of IAS-4 590.5m show marine signatures in the dolomite. The arrow symbol (➡) indicates the results.
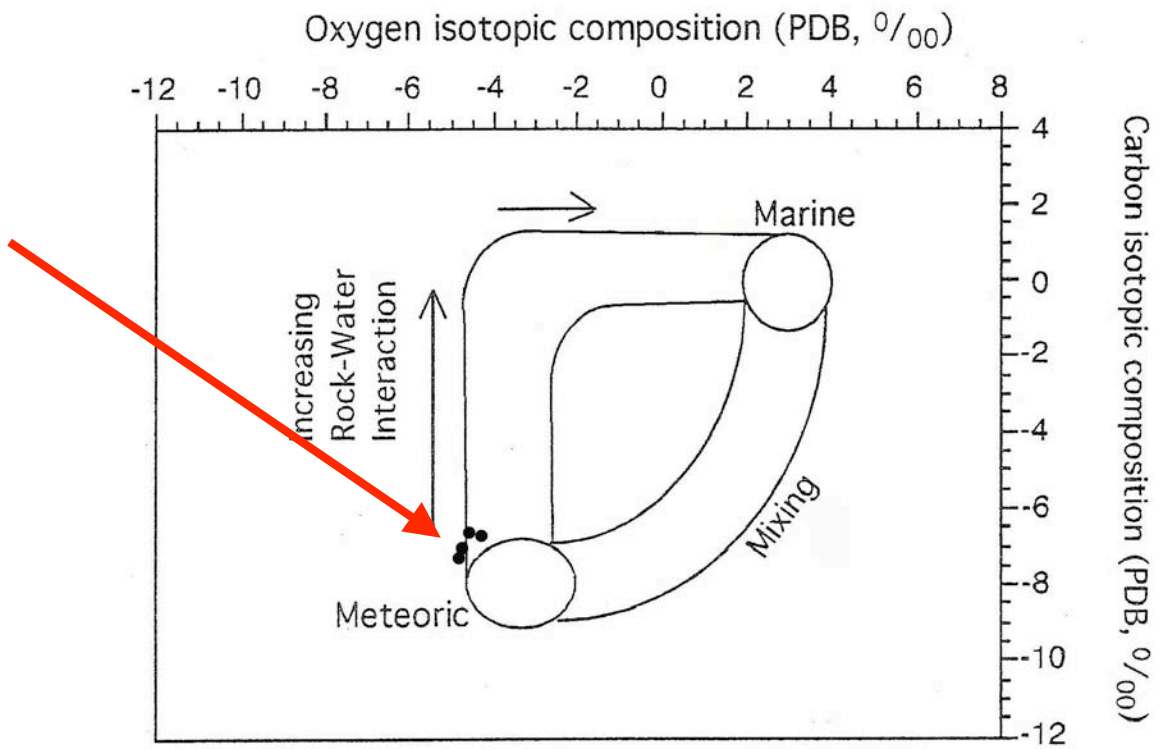
Figure 4.6: Garrochales 522.9m has meteoric water isotopic signatures. The arrow symbol ( ) indicates the zone of results in the graph.
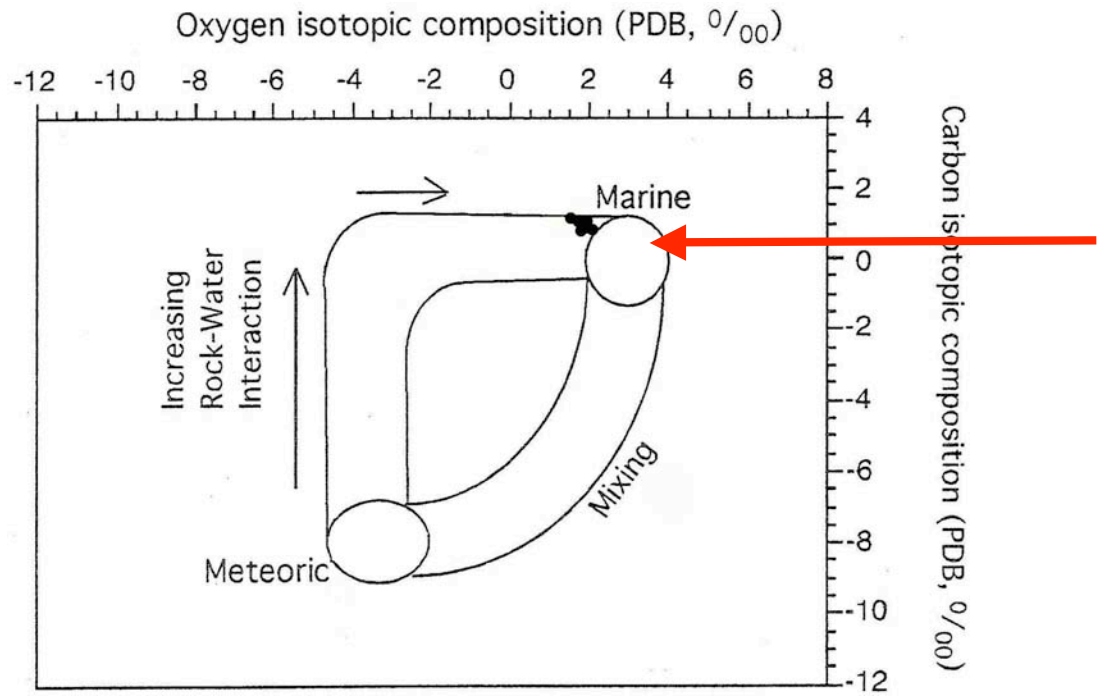
Figure 4.7: IAS-4 420.1m shows marine water signatures.
The arrow symbol (➡) indicates the zone of results in the graph.
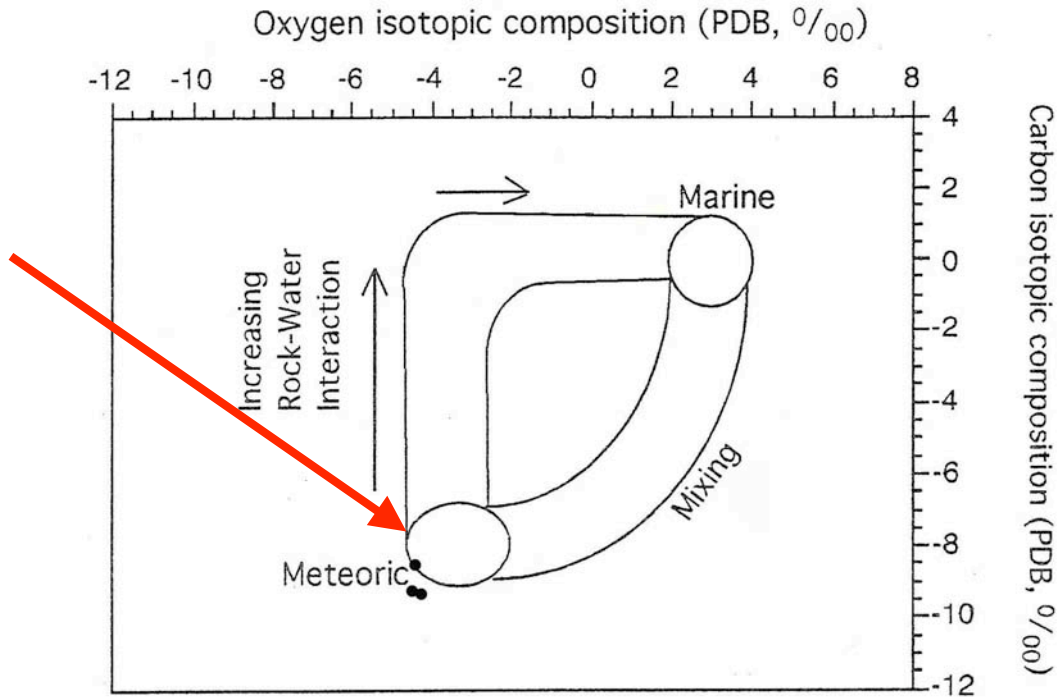
Figure 4.8: NC-10 isotopic analyses have meteoric water signatures. The arrow symbol (➡) indicates the zone of results in the graph.

4.2.2 Stable isotopic analysis in Calcite

Analysis in sample IAS-4 461.3m (calcite) range from 1.20 to 1.68 of $\delta^{18}O$ and 1.08-1.40 in $\delta^{13}C$ (Appendix 1). The data of IAS-4 (461.3m) suggest marine water signatures in the calcite (Figure 4.9). Stable isotopic compositions in the sample IAS-4 420.1m range, from 1.63 to 1.85 $\delta^{18}O$ and 0.76 to 1.20 in $\delta^{13}C$ (Table 4.5) (Appendix 1). This data was obtained from calcite cements and suggest cementation in a marine environment (Fig. 4.10). Stable isotopic compositions in the sample from Garr (522.9 m) range from -4.82 to -4.26 in a $\delta^{18}O$ and -6.89 to -6.13 $\delta^{13}C$ (Table 4.5) (Appendix 1). The samples were obtained from foraminifers, gastropods, and calcite cements. They indicate alteration of the bioclast, in a meteoric environment and cementation in meteoric environment (Fig. 4.11). Stable isotopic compositions in the sample from NC-9 (493.0m) range from $\delta^{18}O$ -3.79 to -0.21 and from $\delta^{13}C$ of -7.18 to -0.76 (Table 4.5) (Appendix 1). The data suggest either alteration in the mixing zone (Fig. 4.12) or rock water interactions. Stable isotopic compositions in the samples analyzed from NC-6 (707.6m) range from $\delta^{18}O$ 0.29 to 0.63 and in $\delta^{13}C$ from -0.37 to -1.45 (Table 4.5) (Appendix 1).

Table 4.5: This table presents the values of stable isotopes in the cores Garr (522.9m), IAS-4 (420.1m), and IAS-1 (685.7m). For the different samples we obtained more than one value to corroborate if the calcite is altered or not.

Samples	δ ^{13}C VPDB	δ ^{18}O VPDB
IAS-4 461.3m	1.40	1.68
	1.08	1.20
IAS-4 420.1m	0.76	1.85
	0.83	1.85
	1.20	1.63
Garr 522.9 m	-6.65	-4.32
	-6.63	-4.64
	-6.89	-4.35
	-6.13	-4.79
	-6.90	-4.40
	-6.94	-4.52
	-6.63	-4.84
	-6.81	-4.82
	-6.43	-4.30
	-6.66	-4.26
Garr 522.9 m	-6.67	-4.41
NC-9 493.0m	-0.90	-0.79
	-8.16	-0.07
	-9.37	0.35
	-7.99	-0.01
	1.19	1.19
	0.87	1.34
NC-6 707.6m	-1.24	-0.21
	-0.47	-0.63
	-1.35	0.43
	-1.45	0.29
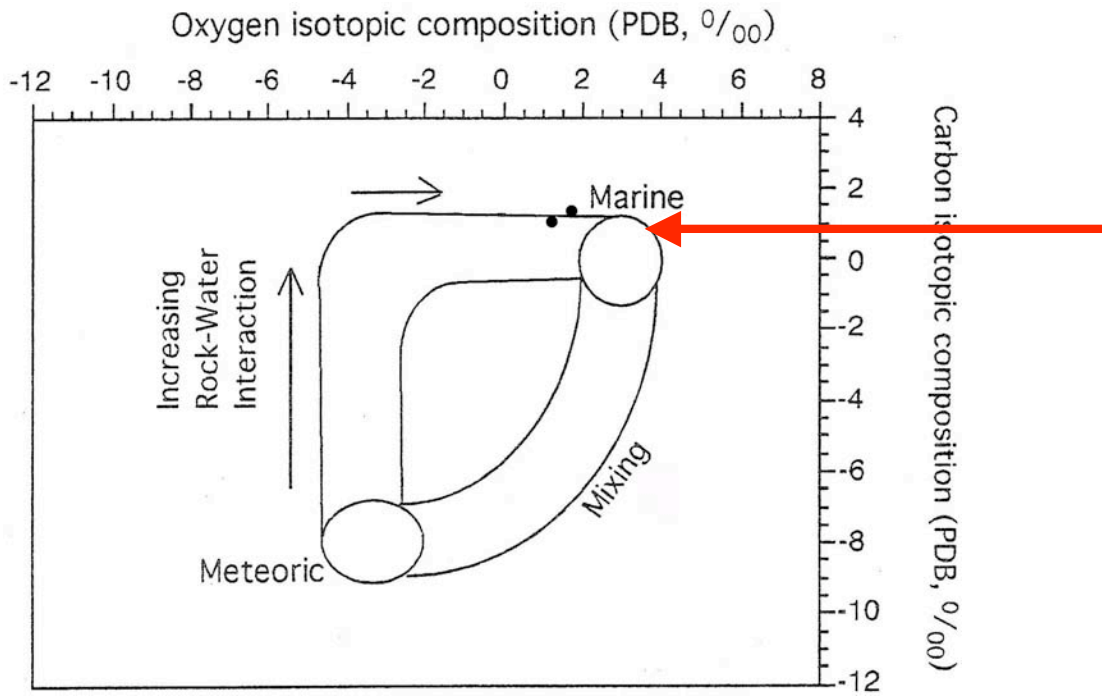
Figure 4.9: Stable isotopic analysis from IAS-4 (461.3m) suggests precipitation of calcite in a marine environment. The arrow symbol (➡) indicate the results.
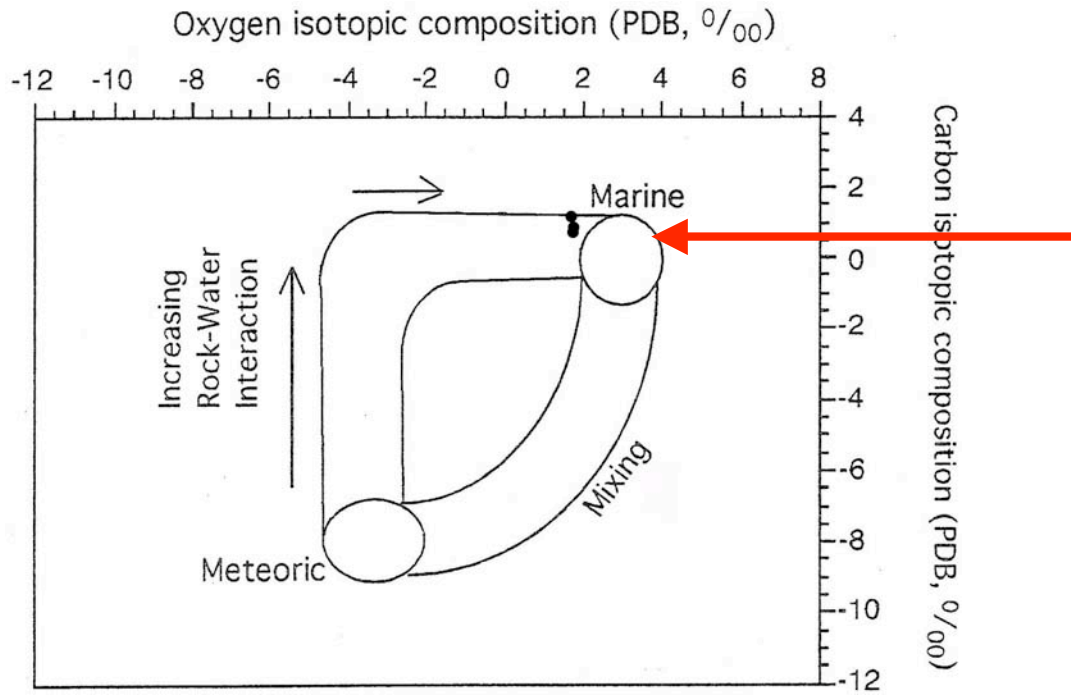
Figure 4.10: Stable isotopic analysis from IAS-4 (420.1m) (calcite) suggest precipitation of calcite in a marine environment. The arrow symbol (⟶) indicates the results.
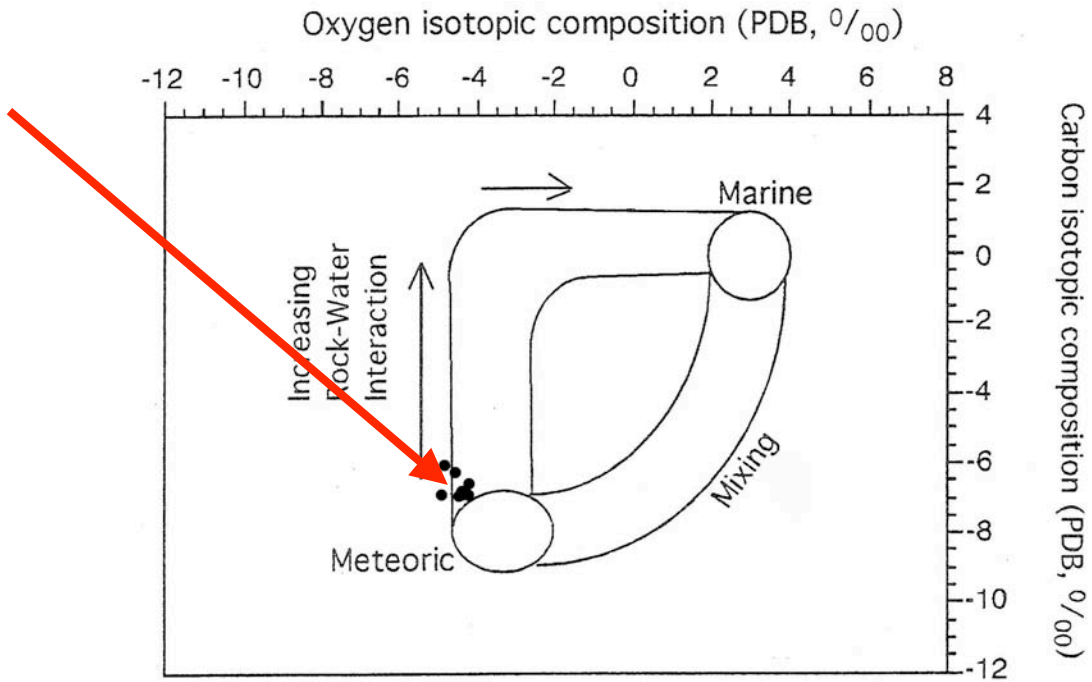
Figure 4.11: Stable isotopic analysis from Garr (522.9m) suggests precipitation of calcite in a meteoric environment or alteration of calcite in meteoric environment. The arrow symbol (➡) indicates results.
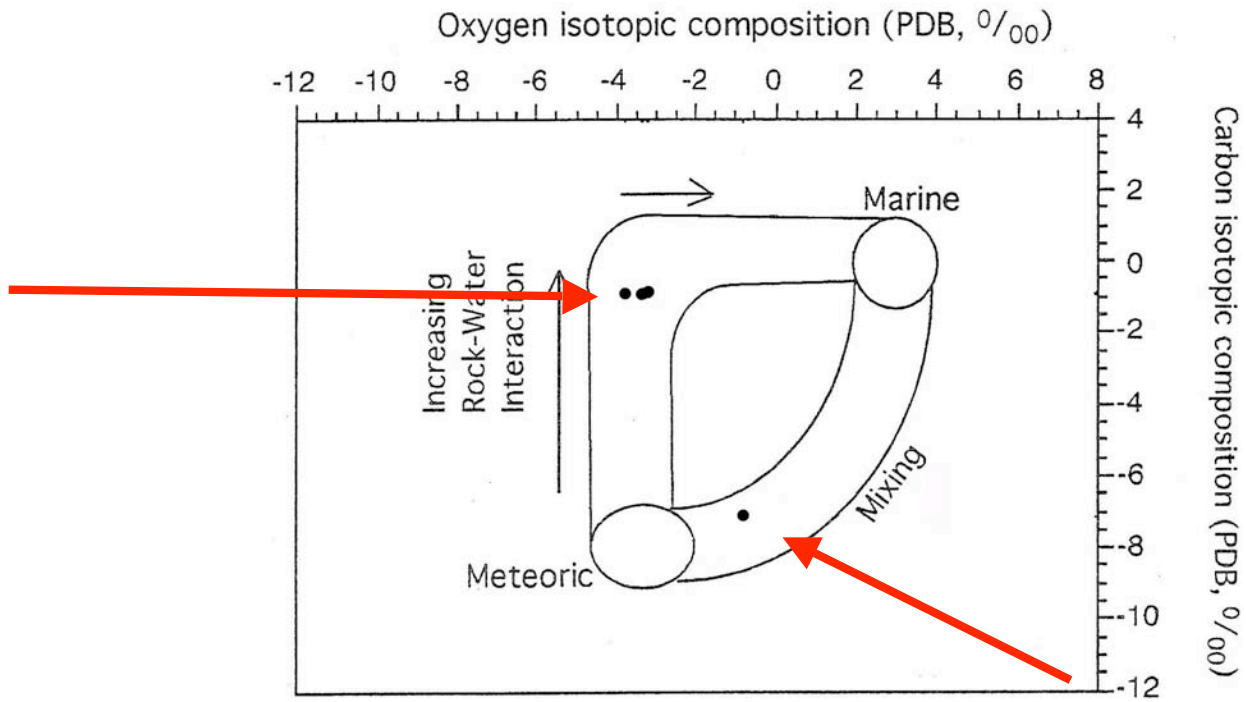
Figure 4.12: Calcite samples in NC-9 core at (493.3m)
suggested host rock interactions and alteration.
The arrow symbol (➡) indicates the results.

4.3 Petrography

To make the fluid inclusions analysis, the most important step is to gather the samples that contain only dolomite. Most samples contained dolomite but also foraminifers or bivalves were abundant. The samples in IAS-4 have 90% dolomite (Fig. 4.13). These samples contain perfect rhombohedral dolomites. Petrography was done to quantify the amount of dolomite and to identify the bioclastic components. Some depositional facies were identified in the dolomites Dolomitized red algae was identified. The abundant bioclats in the samples were the red algae, foraminifers, bivalves, and gastropods. The foraminifers included *Amphistegina* and *Peneroplids*, euhedral dolomites of different grain sizes and styolites (Fig. 4.14) are also present. The most abundant porosity type in the samples were moldic and intercrystalline. Some bioclasts have been dolomiticized. The bivalves, foraminifers, and some cements in the samples contain the mineral calcite. Some euhedral calcite crystals are present inside crystals of dolomite that are partially dissolved (Fig. 4.15). The dolomites have been definitively dedolomitization after crystallization (Fig. 4.15). The dissolution of the crystals of dolomite and the dolomite cements is evidence that indicated their alteration. This evidence suggested that dolomites have been altered after deposition.
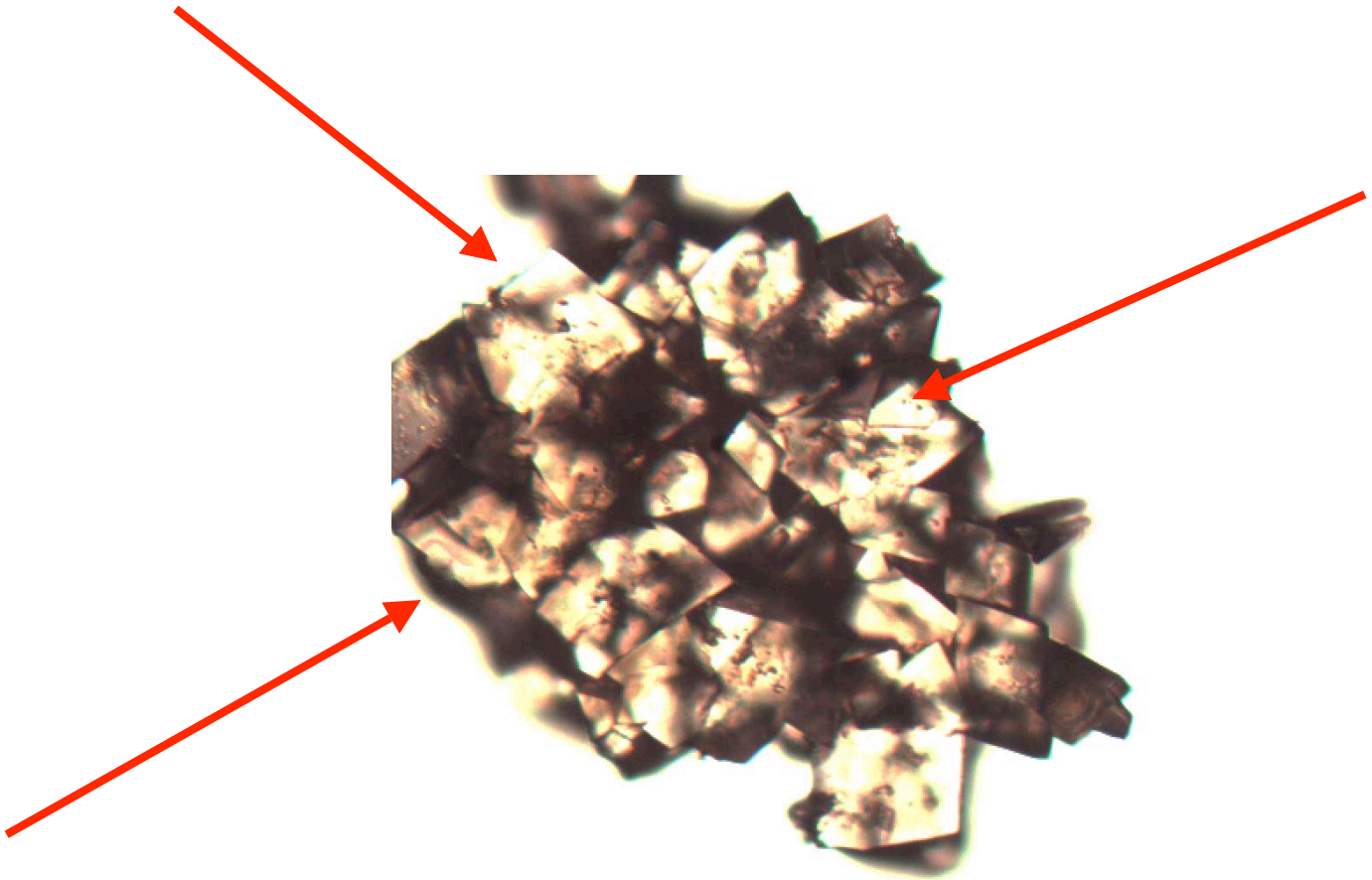
Figure 4.13: Samples IAS-4, 420.1m shows rhombohedral dolomite. The arrow symbol
(➡) shows the crystals.
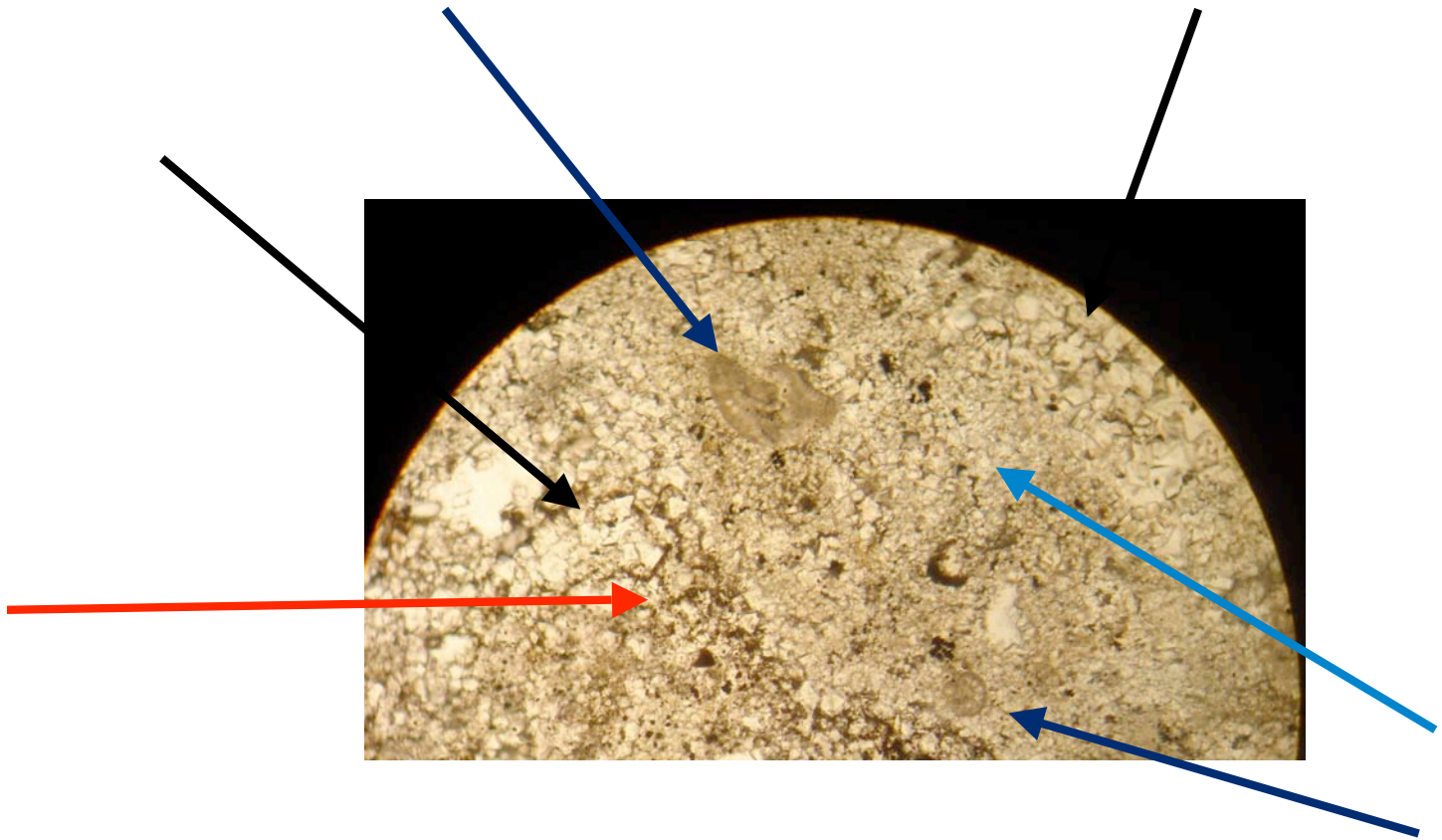
Figure 4.14: Different type of foraminifers and different crystal sizes of dolomite and styolite in the sample IAS-4. The red arrow (➡) indicates the styolite, the black arrow ◀▶) indicated the big crystals of dolomites, the blue arrow (▶) indicate small crystals of dolomite (➡) indicate the foraminifers.
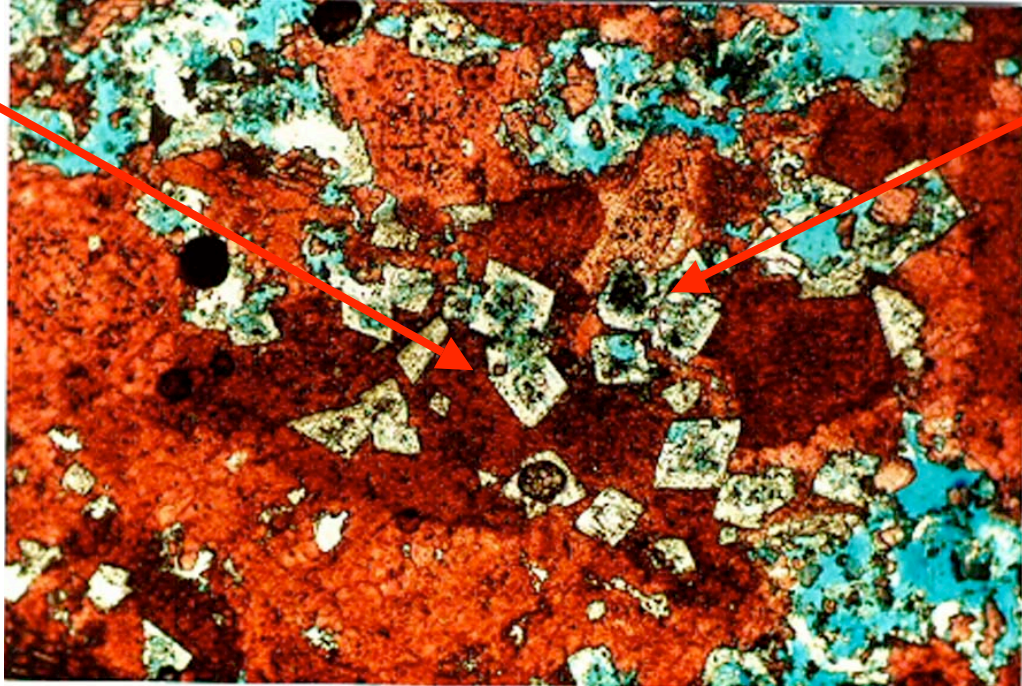
Figure 4.15: NC-5 core at -3.82.2m. Dissolution of dolomites that replaced calcite bioclasts. These dolomites are stratigraphically high in the study area. Calcite cement inside the dissolved dolomite rhombs indicate post dolomite precipitation.

Chapter 5

Discussion

5.1 Discussion of the fluid inclusions analyzes

As discussed in Chapter 1 there are four models of dolomitization all based in the alteration of seawater. The models of dolomitization explain how the dolomites precipitated in different environments and the factors that are involved in their precipitation. Models based on the evaporation of seawater and models based on marine water dolomitization have been ruled out of the Puerto Rico north coast dolomites. No evaporates have been described for the geology of the north coast. The model that best fit the precipitation of the dolomites in the north coast is the mixing zone model that proposes the mixing of seawater with freshwater creating the dolomitization fluid (Chapter 1).

A fluid inclusion analysis can help to identify the fluids associated with the precipitation of rocks or minerals (Fig. 5.1). In this study, samples of dolomites were analyzed for fluid inclusions. To determine the salinity and the precipitation environment suggested by the fluids in the dolomites, the final temperature of homogenization was used. The final temperature of homogenization from the samples of Montebello Member (Cibao Formation) for IAS-4 (510.1m) were 0.00 to 0.01 and for IAS-4 (590.5m) was 0.00 (Chapter 3). The equations established by Hall et al. (1988) provided the salinity of the fluid present in the fluid inclusions based on the final temperature of homogenization that was measured. Table 3.2 of Bondar (1992) was also used to obtain the salinity of the fluids that corresponds to a freezing temperature for a temperature between 0.0 to -21.2°C. According to the table and according to

the equations the inclusions in the studied dolomites are composed of freshwater. A final

temperature of homogenization of 0.01 indicated only a small quantity of salt in the fluids, but

according to the equations and tables 4.2 and 4.3 this is still freshwater. This sample was taken

at Montebello Member (Cibao Formation) at IAS-4 (510.1m). The stable isotopic signatures of

the samples IAS-4 (510.1m) indicated marine water was present during dolomitization. The

value of strontium in the sample of IAS-4 (510.1m) is 0.708326 (Ramirez, 2000). This value of

$^{87}Sr/^{86}Sr$ suggests a timing of dolomitization similar to marine deposition of the Lares

Limestone and Montebello Member of the Cibao Formation. The values of $^{87}Sr/^{86}Sr$ indicated

contamination of the Sr isotopic fluids or recrystallization of the dolomite. The strontium

isotopes and the fluid inclusions analysis in the samples of the Montebello Member at IAS-4

(510.1m) both suggest a possible recrystallization of the dolomite.

Fluid inclusions can be trapped during the process of recrystalization in diagenetic

minerals. The inclusions that are present during the process of recrystallization provide the

record of the conditions of recrystallization rather that the original precipitation of the mineral.

The cavity that occurs during the process of recrystallization provides the conditions and is

recorded in the minerals during this process. Most of the fluid inclusions studied in the

dolomites of the north coast of Puerto Rico seem to have been trapped during the process of

recrystallization. Since dolomitization cannot occur in freshwater, the freshwater in the fluid

inclusions must have been collected some time after dolomitization during the recrystallization

of the already formed dolomite.

The freshwater data obtained for the fluid inclusions of Montebello Member (Cibao

Formations) at IAS-4 (510.1m) and (590.5m) indicate the environments where dolomites have

been recrystallized. The data of freshwater and the small quantity of salt may be a remanent of

fluid where the dolomites were originally precipitated. This small amount of salts present in sample supports a mixture of fresh and saltwater during dolomitization. The fluid inclusion data showing freshwater suggest that recrystallization occurred in a freshwater (aquifer) environment. This assesement is consistent with the geologic history and of rocks that are today present in the aquifer system.

The stable isotopic data obtained in the study supports the recrytsallization hypothesis. Samples from the Montebello Member and Lares Limestone cores IAS-4 (510.1m), (590.5m), and (420.1), NC-9 (493.3), Gar (522.9) show meteoric environments. This supports that the dolomites were originally precipitated in a different environment and later recrystallized in a meteoric environment. The presence of calcite inside dissolved dolomites indicates their alteration. The calcite cements present after the dolomite cements in the paragenetic sequence indicate that a freshwater environment followed dolomitization. Also the presence of dedolomitization identified by the petrographic analyses (Fig. 4.15) indicates that the dolomites have reacted in the recent environments after they were formed. All these evidences points to the fact that the dolomites may have been altered.

The geologic history of the rocks shows that a freshwater environment followed the dolomitization. During the late Oligocene to Miocene and early Pliocene there was a time of eustatic drop of sea level and tectonic uplift combined with subsidence in the northern part of Puerto Rico (Renken,2002). This caused the intrusion of the meteoric water in the limestone creating, first mixing zone and later extensive aquifers by the expulsion of the marine water that was in the rocks before this event (Renken, 2002). An exposure during the Middle Miocene of the Aguada and Aymamón Limestone is evidenced by an unconformity and resulted in the input of fresh water in the aquifer producing a freshwater digenetic environment that followed the

dolomitization (dolomitization occurred in the late Oligocene-early Miocene according to Ramírez, 2000). This process of tilting, uplift and sea level fall produced enough hydraulic head to gradually flush all the marine water out of the rocks. Initially this meteoric water invaded the aquifer in the shallow areas creating mixing zones but later it also invaded the deeper down dip parts of the Lares Limestone and Montebello Member of the Cibao Formation (Middle Miocene) (Renken, 2002).

The stable isotopic compositions of samples from the Montebello Member at Cibao Formations at IAS-4 at depths 420.1m, 590.5m and 461.3m have meteoric water signatures with rock water interaction influences. All these data is consistent with the geologic history proposed by Renken (2002) for the Lares Limestone and the Montebello Member that discussed above.

The stable isotopes in calcite in the Montebello Member and the Lares Limestone in the cores IAS-4 (461.3m), (420.1m), Garr 522.9m and NC-9 (493.3) showed meteoric and marine water signatures. The stable isotopic signatures obtained from blocky calcite cement precipitated after the dolomite in the paragenetic sequence (Fig. 4.15) suggest precipitation from a meteoric fluid and exposure to freshwater environments.

The $^{87}Sr/^{86}Sr$ compositions measured in the Puerto Rico north coast modern artesian aquifers range from 0.7089 to 0.7088 (Román Más et al., 1988). This is no surprise since the Sr is coming form the rock that form the aquifer and these were deposited during Oligocene to early Miocene times. The dolomitization ages obtained from $^{87}Sr/^{86}Sr$ coincide with the marine waters present during the deposition of the Lares Limestone and the Montebello Member of Cibao Formation. This would imply that the dolomitization ocurred at the same time of the deposition of the units. The dolomites could not have been produced at the same time or during the deposition of the host rock because they are replace (diagenetic) dolomites. Based on this

assessment the $^{87}Sr/^{86}Sr$ has been contaminated during recrystallization of the dolomites. The most probable source of $^{87}Sr/^{86}Sr$ contamination would be the $^{87}Sr/^{86}Sr$ in the meteoric (aquifer) waters of the Lares Limestones and Montebello Member. It is expected that the $^{87}Sr/^{86}Sr$ in this aquifer waters would be very similar to the $^{87}Sr/^{86}Sr$ of the aquifer rocks due to rock-water interaction processes. Contamination of aquifer waters (meteoric-aquifer) with rations of 0.708199 to 0.708295 (ratios developed by the rock-water interaction) during the dolomite formation or during recrystallization would have produced ages of dolomitization older that the correct ones and directly related to the ages of the aquifer bearing rocks. This seems to be the case since the ages of dolomitization overlapped the ages of the deposition of the rocks. If this reasoning is true the Sr isotopic composition cannot be used to determine the age of dolomitization (Fig. 5.3). However it can be used to imply that the dolomites have been altered by recrystallization in aquifer waters, a fact that has been supported by our fluid inclusion analysis and our stable isotopic analysis. In other words, the Sr isotopic study by Ramírez (2000) can be used as another line of reasoning and evidence that points to the recrystallization of the dolomites in a freshwater-aquifer environment. It is important to point out that this contamination of Sr isotopes could also be used to support dolomitization in a mixing zone environment suggesting that the fluid was a mixture of marine and aquifer water.

Trace elements are incorporated into a mineral or solid solutions and can substitute the Ca^{+2} in the dolomite structure. High Sr/Ca concentrations in the dolomites indicate marine water or predominantly marine water (Ramírez, 2000). In marine dolomite the concentration of Sr is expected to vary from 0.039 to 0.048 (that represents 600 to700 ppm of Sr; Appendix VII). The concentrations of Sr^{+2} that Ramírez, (2000) obtained in the dolomites (0.70859 to 0.708276, Ramírez) represent marine water.

The concentration of Fe in seawater is 0.002ppm. Ramírez (2000) measured the dolomite concentration of Fe to be of 0 to 846ppm (Appendix VI). This suggests that these dolomites were either precipitated from altered marine water or were altered in non-marine conditions. The concentration of Mn and Sr/Ca also suggests the possibility that the dolomites were altered in meteoric environments (Ramírez, 2000) or precipitated in a mixture waters.

Most of the data obtained in this work is combined with data of Ramírez (2000) and can be used to support dolomite alteration in a meteoric environment regardless of what was the initial dolomitization environment. This model best fit the petrography and geochemistry of the dolomites with the fluid inclusions data produced in this study. Although some of the results (the trace elements, stable isotopic, and Sr isotopic analysis) can be explained by a mixing zone dolomitization environment as well as by recrystalization of the dolomites after their formation. Fluid inclusion analysis (which is the primary focus of this project) point to the fact that the dolomites have been altered after they were formed.
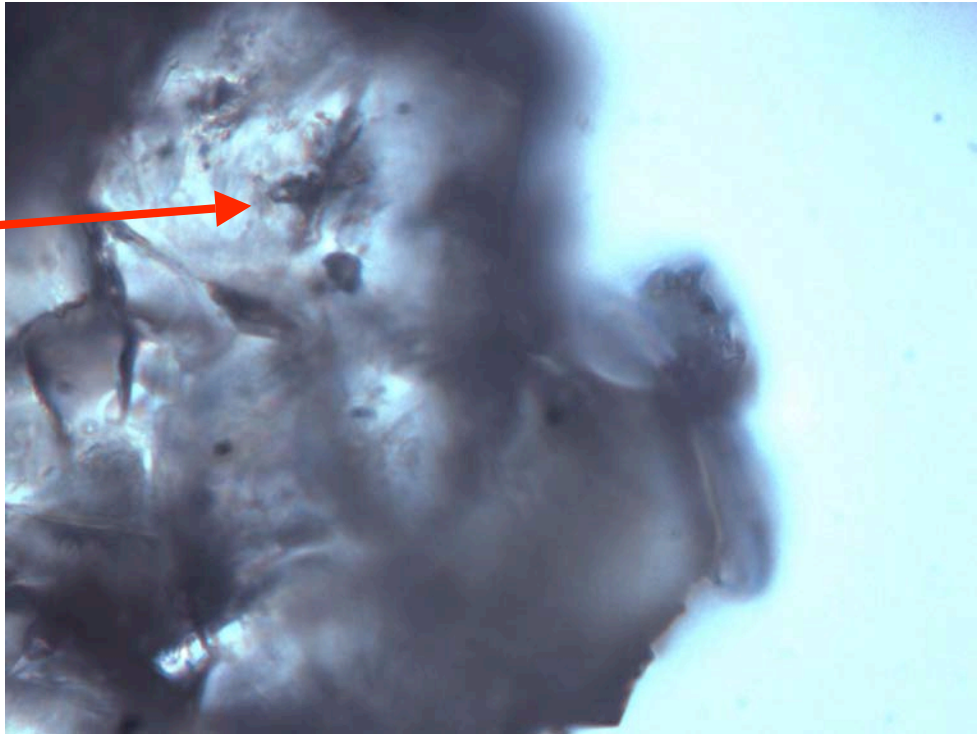
Figure 5.1 Samples of fluid inclusions IAS-4, 510.1m.

middle to late Miocene

meteoric water input

Eustatic Sea Level Fall

impermeable

impermeable

marine water

meteoric water input

impermeable

impermeable

marine water

Eustatic Sea Level Rise
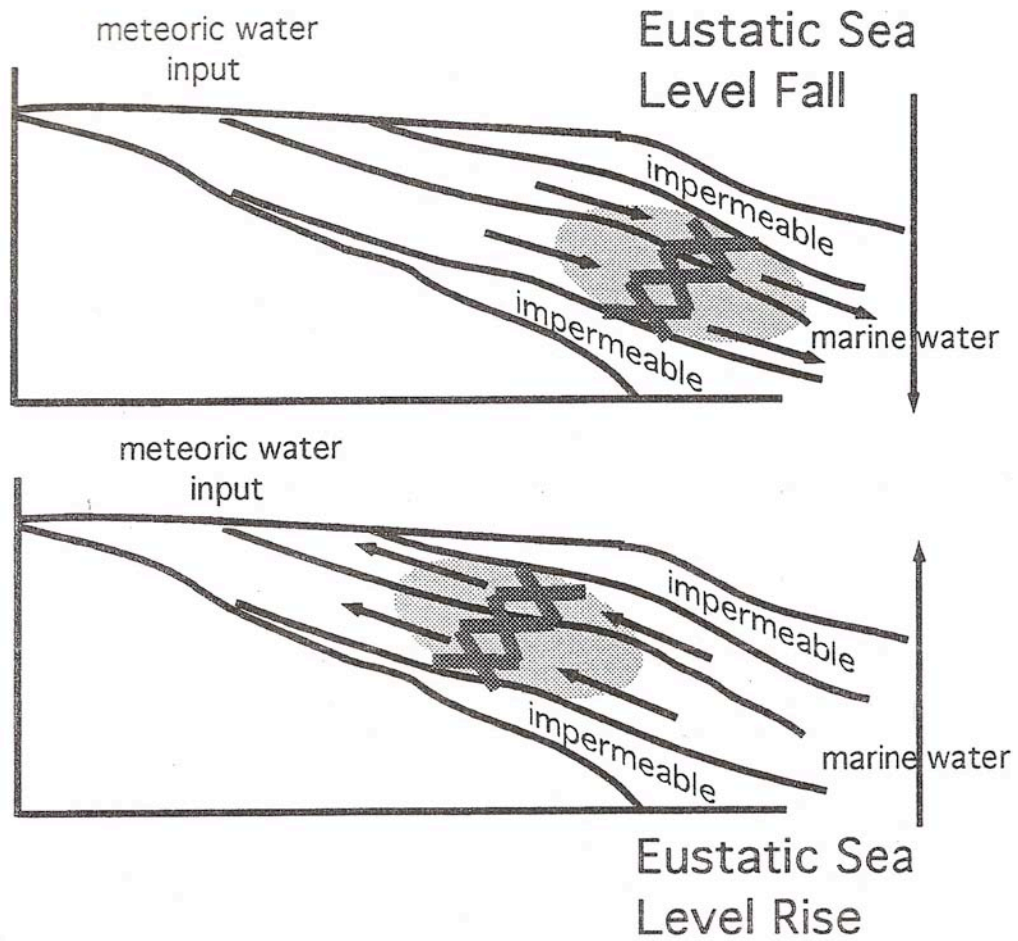
Figure 5.2 Eustatic sea level changes could have provided the flow and
movement of the mixing zone causing the dolomitization
of extensive stratigraphic intervals (Ramírez, 2000).
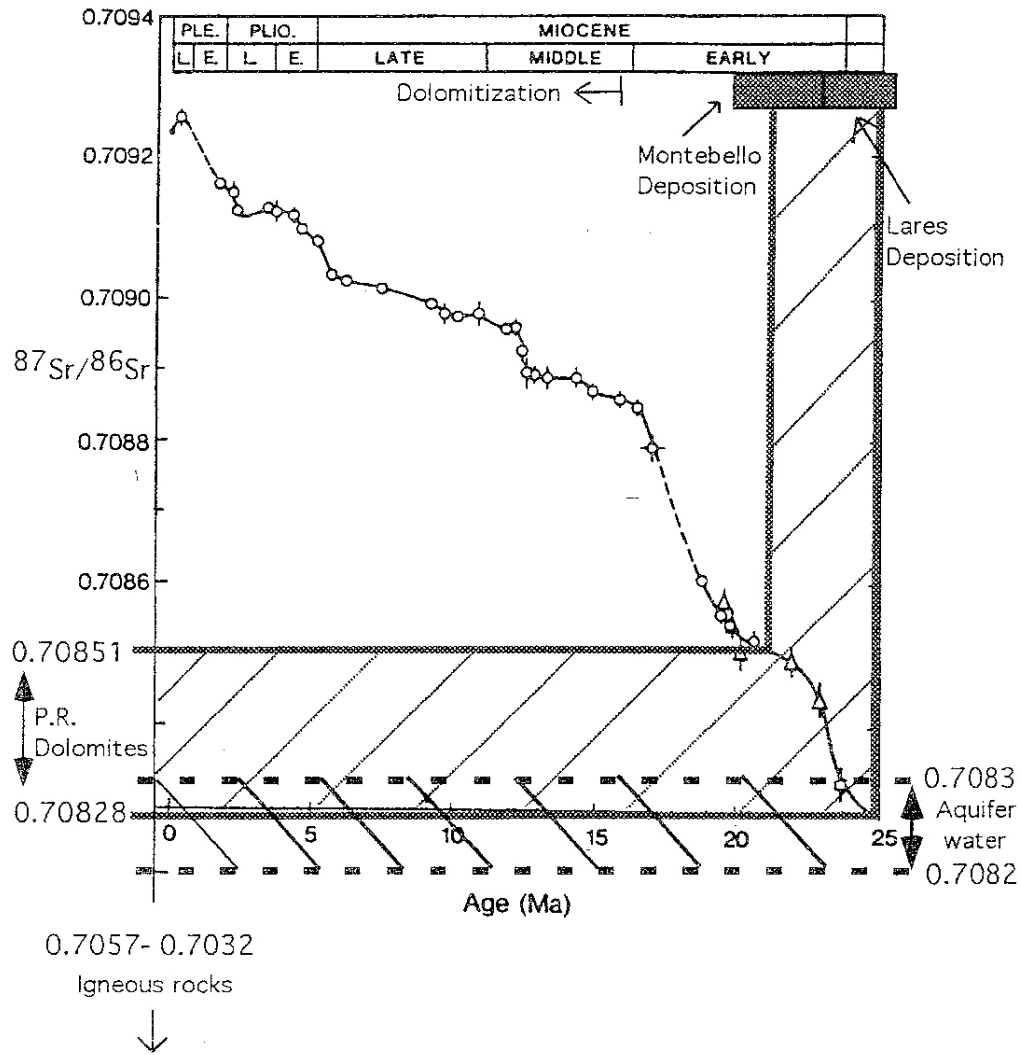
Figure 5.3: Strontium isotopic values of the dolomites compared with the aquifer, marine and ignesous rock values (from Ramírez, 2000). The values obtained suggest alteration of the Sr isotopic signatures in waters produced by rock-water interaction in the host aquifer rocks. The Sr isotopes in the dolomites are very similar to the Sr isotopic values of the host rocks were dolomitization occured. The Sr values obtained would imply that dolomitization and deposition of the limestones occurred at the same time and this is imposible especially for replacive dolomites as the ones studied.

Chapter 6

Conclusions

The stable isotopic analysis in the dolomites (Garrochales, IAS-1 and NC-10) suggests either alteration of the dolomites in meteoric waters and/or original crystallization in a mixing zone environment. The stable isotopic data for the calcite (IAS-4 461m), (IAS-4; 420.1m and Garr; 522.9m) suggests precipitation of calcite in a marine environment, meteoric water and also produced rock water interactions. The data clearly shows that an heterogeneous environment between meteoric and marine waters has been present in the rocks during their history. This environment is consistent with the geologic history of the rocks in the area were a progresion from marine to mixing (marine-meteoric) to finally a meteoric environment seem to have occurred.

The inclusions measured in the dolomites studied are composed of freshwater. Only one sample showed a small quantity of salt but it is still in the freshwater field. This fluid inclusion, if primary, would support the mixing zone dolomitization model proposed by Gonzalez and Ruiz (1991) and Ramírez, (2000). However the result is not conclusive since this is only one data point and the salt concentration is low. Since dolomitization has never been reported to occur in freshwater, neither in nature nor in laboratory experiments, the inclusions present in the dolomites most probably provide a record of the fluid present during recrystallization rather than the fluids present during the original precipitation of the dolomite. Dedolimitization textures (Fig. 4.15) present in the dolomites show that alteration has affected the dolomites and support this assessment.

Reference:

Alonso-Harris, R. Krieg, E.A., and Meyehoff A, 1983, Post-early Pliocene age of
Puerto Rico Trench: Caribbean do Indes, Geological Conference, 10th Cartagena
Columbia, Abs p.148.

Arredondo G.S.G., Muneton, G.M., Zenteno Morán, D.J., Nishirura Grajales J.M., Ibarra
And Schaaf P., 2007, High Temperature dolomites in the lower Cretaceous Cupido
Formation, Bustamante Canyon, northeast Mexico: petrologic, geochemical and
microthermometric constrains, Revista Mexicana de Ciencias
Geologicás v.24, num 2, p.131-139.

Badiozamati, K. 1973, The Dorag dolomitization model-Application to the Middle
Ordovician of Wisconsin, Journal of Sediments Petrology, v.43, 4 p.965-984.

Berkey, C.P. 1915, Geological reconnaissance of Puerto Rico: New York. Academy of
Science Annuals, v.26, p.170.

Bermúdez, P.J., and Seiglie, G.A., 1970, Age, paleocology, correlation and foraminifers of the
Uppermost Tertiary formation of northern Puerto Rico: Caribbean Jour. Sci., v10, nos.
1-2, p. 17-33

Bilich, A., Frohlich, C., and Mann, P., 2001, Global seismicity characteristics of subduction to
strike-slip transitions: Journal of Geophysical Research, v.106, p. 19,443-19,452, doi:
10.1029/2000JB900309

Birtch, G.S. 1986, Isostatic, thermal and flexural models of the subsurface of the
North Coast of Puerto Rico: Geology V.14 p.427-429

Bodnar, R.J., 1922 a, Revised equation and table for freezing point depression of H_2O-
Salt fluid inclusions (Abstract): PACROFI IV; Fourth Bienniel Pan-American
Conferenc on Research of Fluid Inclusions programs and abstracts Lake Arrow
Head, CA, v. 14 .15

Bodnar, R.J., 1922 b, The system H_2O-NaCl (Abstract): PACROFI IV, Fourth Bienniel
Pan-AmericanConferenc on Research of Fluid Inclusions programs and abstracts Lake
Arrow, CA. v 4 p.108-111

Brantley, S.L., Evans, B., Hickman, S.H. and Cerar, D.A., 1990, Healting of microracks
in quartz implications for fluid flow: Geology, 18, p.136-139

Brantley, S.L., 1992, the effect of fluid chemistry on quartz microcrak lifetimes: The
Earth and planetary Science Express 145

DeMets, C., Jansma, O., Mattioli, G., Dixon, T., Farina, F., Bilham, R., Calais, E., and Mann, P., 2000, GPS geodetic constraints on Caribbean-North America plate motion: Geophysical Research Letters, v. 27, p.437-440

Frost, S.H. Harbour, J.L. Beach, D.K., Realini, M.J. and Harrig P.M. 1983, Oligocene tract development southwestern Puerto Rico sediments IX, p.144

Giusti, E.V., 1978, Hydrogeology of the Karst of Puerto Rico, U.S. Geological Survey Professional Paper 1012, 68

Goldstein H.G. and Reynolds T. J., 1994, Systematic of fluid inclusions in diagenetic minerals

González L.A., Ruiz H., 1991, Diageneis of Middle Tertiary in the Toa Baja Well, Puerto Rico, Vol 18, NO3, Page-513-516

Hardie L.A., 1986, Dolomitization a critical view of some current views. Department of Earth and Planet Sciences, The Johns Hopkins University. Baltimore Maryland 21218.

Hartley, J.P. 1989, Subsurface Geology of the Tertiary carbonate rocks, northwestern Puerto Rico: [unpub. M.S. thesis]: University of New Orleans, p.214

Holand, H.P., 1964, Solubility of calcite in NaCl solution between 50° and 200°C (abs): Geological, Society America spec. paper 82, p. 94-95

Hubbard, B, Hubbard, B, . 1923, The Geology of the Lares district, Puerto Rico, New York Academy of Science, V2, p-1-115

Land L. S., 1982, Dolomitization: A.A.P.G. Education Course Note Series, 24, p.1-5

Lyman, J. and Fleming, R.H., 1940, The composition of seawater, Journal of Marine Research, v.3, p.1340146

Lohmann, K.C., 1982, Inverted J Carbon and Oxygen isotopic trends-criteria for Shallow meteoric phreatic diagenesis: Geological Society Amen: Abstract With programs, p.548.

Machel H. G., 2000, Dolomite Formations in Caribbean Islands Driven by Plate Tectonics, Vol 70 No 5, p.977-984

Mann P., Prentice, C.S., Burr, Pe   a, L.R., and Taylor, F.W., 1998, Tectonic geomorphology and Paleoseismology of the Septentrional fault system, Dominican Republic, in Dolan, J.F., And Mann, P. eds., Active strike-slip and collisional tectonics of the Northern Caribbean Plate Boundary Zone: Geological Society of America Special Paper 326, p.63-123

Mann P., and Burke, 1984 Neotectonics of the Caribbean: Reviews of Geophusics and
Space Physics, v22, p.309-362

McCann, W.R., 2002, Microearthquake data elucidates Caribbean subdcution zone:
Seismologocial Resarch Letters, v.73, p.25-32

Matos, R., 2000, Controls on porosity in the North Coast Aymamón limestone: [unplub.
M.S. thesis]: University of Puerto Rico at Mayaguez, 85p.

Matteos, R.K., 1971, Diagenetic environments of possible importance for the explain
Mattson, P.H., 1984, Caribbean Structural breaks and plate movements: G.S.A
Memoir, 162 p. 131-153

Mattson, P.H., 1984, Caribbean structural breaks and plate movements: G.S.A. Memoir
162, p. 131-153.

Meyerhoff, H.A., 1975, Stratigraphy and petroleum possibilities of Middle Tertiary rocks
in Puerto Rico: discussion, A.A.P.G. V.59, p.169-172

Meyerhoff, H.A.,Krieg, E.A., Closs, J.D. and Taner, I., 1983, Petroleum potential of Puerto Rico,
Oil and Gas Journal, v. 81, p, 113-120.

Monroe, W.H., 1962, Geology of the Manatí quadrangle Puerto Rico, U.S. Geological Survey,
MAP GQ-197, scale 1: 20,000.

---------1963 Geology of the Camuy Quadrangle, Puerto Rico, U.S. Geological Survey, MAP
GQ-197, scale 1: 20,000.

---------1968, The Aguada Limestone of Northwest Puerto Rico: U.S.G.S. Bull,
Bull 1274-G, p.G1-G2

---------1980a, Geology of the Middle Tertiary Formations of Puerto Rico:
U.S.G.S. Profesional Paper, 953, p.39

Moussa, M.T., and Seiglie, G.A., 1975, Stratigraphy and petroleum possibilities of middle
Tertiary rocks in Puerto Rico: discussion, Am. Assoc. Petroleum Geologits, vol.59,
p.163-168

Moussa M. Seigle,G., Meyerhoff, A. & Taner, I., 1987, the Quebradillas Limestone (Miocene-
Pliocene), northern Puerto Rico, and tectonics of the northeastern Caribbean margin.
Geological Society of America Bulletin, v.99 , p.427-439

Nelson, A.E., 1966, Cretaceous and Tertiary rocks in the Corozal Quadrangle, northern Puerto
Rico: U.S. Geol. Survey Bull, 1244-C, p.C1-C20

Pecher, A., 1981, Experimental decrepitation and reequilibration of fluid inclusions in synthetic

Quartz: Tectonophysics, v.78 p. 597-583

Pinell, J.L., Dewey, J.F., 1982, Permo-Triassic of western Pangea and the evolution of
the Gulf of Mexico/ Caribbean region, Tectonics (1), 179-211

Prentice, C.S., Mann, Pe a, L.R.., and Burr, G., 2003, sli rate and earthqueake recurrence along
the central Septentrional fault, North American-Caribbean plate boundary, Dominican
Republic: Jpurnal of geophysical Research, v. 108 *B3), doi 10.1029/2001HB000442

Ramírez W., 2000, Dolomitization and evolution of the Puerto Rico
North Coast confined aquifer system: [unpub. M.S. thesis]: Ph.D. Thesis,
Tulane University

Renken, R.A., Rodríguez-Martínez J., and Gómez-Gómez, F, 2002, Hydrogeologic
Framework of the U.S. Caribbean Islands in : Renken R.A. and others, Geology
and Hydrogeology of the Caribbean Islands Aquifers System Commonwealth of
Puerto Rico and Unite States Virgin Islands: United States Geological Survey
Paper 1419

Rodríguez M., J. 1995, Hydrogeology of the North Coast Limestones
Aquifer system of Puerto Rico: U.S.G.S. Water Resources Investigators,
Report 94-4229, p. 22

Roedder E., 1984, Fluid Inclusions, Volume 12, Mineralogical Society of America p. 13, 20, 22

Román-Más A., and Lee, R. W. 1987, Geochemical evolution of waters within the north
Coast limestone aquifers of Puerto Rico: A conceptualization based on a flow
Path in the Barceloneta area: U.S.G.S. Water- Resources Investigations Report,
86-4080, p.28

Scharlach, R. A, 1990, Depositional History of Oligocene-Miocene carbonate rocks,
subsurface of Northeastern Rico: [unplub. M.S. thesis]: University of New
Orleans. 242p.

Seigle , G.A., and Moussa, M.T., 1984, Late Oligocene-Plicocene trangressive-regressive
cycles of sedimentation in northwestern Puerto Rico, in Interregional
unconformities an hydrocarbon accumulation edited by Scheele, J.S. American
Association of Petroleum Geologist memoir 36, p.89-95

Siemiers, W.T. and Ahr, W.M., 1990, Reservoir facies pore characteristics of cyclical
Mixed carbonate-clastic gas reservoirs Lower Permian Chage Group, Cymon-
Hugoton Field Oklahoma (Abstract): American Associations of Petroleum
Geologits, Bulletin, v 74, p.763

Soto D. J., 2009, Analysis of the Lares Limestone Carbonate Sequences exposed on the
    Road Puerto Rico #111, Between km 27.1-27.5

Tucker, M. & Wright V.P., 1990, Carbonate Sedimentology Chapter 2, p. 28-67
    Blackwell Science Ltd, Uk.

Ward, W.C. Scharlach R.A. & Hartley, H.R., 2002, Geology of North Coast
    ground-water province of Puerto Rico. U.S. Geological Survey, Professional Paper 1419,
    p. 45-76

Zapp, A.D., Berquist, H.R. and Thomas, C.R., 1948, Tertiary geology of the Coastal
    Plains of Puerto Rico: U.S.G.S Oil and Gas Investigation Preliminary Map 85

APPENDIX I: DOLOMITE STABLE ISOTOPE ANALYSIS

Identifier 2	1 Cycle Int Samp 44	1 Cycle Int Ref 44	Δ mV	δ ^{13}C VPDB	δ^{13}C/^{12}C Std Dev	δ ^{18}O VPDB	δ^{18}O /^{16}O Std Dev
Sample Notes:			Northcoast dolomites P.R.				
Data File:			080410_KIEL_GC_M.Torres_Northcoast P.R._a				
Calcite	3558	3690	-3.6%	-6.77	0.01	-4.41	0.03
Dolomite	3398	3503	-3.0%	-6.72	0.01	-4.33	0.00
Calcite	3662	3712	-1.3%	-0.90	0.01	-3.43	0.02
Calcite	3069	3129	-1.9%	-0.87	0.00	-3.41	0.01
Calcite	3728	3860	-3.4%	-0.76	0.01	-3.30	0.01
Calcite	3351	3351	0.0%	-0.80	0.01	-3.34	0.02
Calcite	3840	3887	-1.2%	-0.87	0.01	-3.79	0.02
Calcite	3293	3375	-2.4%	-1.24	0.01	-0.21	0.01
Calcite	3281	3257	0.7%	-0.47	0.01	0.63	0.02
Calcite	2984	2982	0.1%	-1.35	0.01	0.43	0.01
Calcite	3527	3663	-3.7%	-1.45	0.01	0.29	0.02
Calcite	3828	3892	-1.6%	-9.35	0.01	-4.39	0.02
Calcite	2496	2511	-0.6%	-9.82	0.01	-4.62	0.02
Dolomite	2736	2741	-0.2%	-9.31	0.01	-4.53	0.02
Dolomite	3611	3671	-1.6%	-9.41	0.01	-4.37	0.02
Dolomite	3000	3033	-1.1%	-9.28	0.01	-4.45	0.03
Calcite	3603	3757	-4.1%	-9.29	0.01	-4.62	0.01
Calcite	3340	3461	-3.5%	-0.19	0.01	-0.76	0.01
Calcite	3491	3469	0.6%	-0.14	0.01	-1.06	0.01
5calcite	4564	4861	-6.1%	-0.09	0.01	-0.74	0.02
Calcite	3272	3348	-2.3%	-0.10	0.01	-0.78	0.01
Dolomite	3285	3309	-0.7%	0.04	0.01	-0.39	0.01
C/D	1561	1560	0.1%	-0.20	0.02	-0.91	0.03
C/D	1363	1337	1.9%	0.07	0.02	-0.34	0.03
Dolomite	4399	4575	-3.8%	-0.09	0.01	-0.86	0.01
Dolomite	2729	2692	1.4%	-0.01	0.01	-0.55	0.01
Ext. std	3396	3405	-0.3%	-5.69	0.01	-3.75	0.01
Ext. std	3829	3987	-4.0%	-5.81	0.01	-3.67	0.01
Ext. std	4135	4267	-3.1%	-5.88	0.01	-3.65	0.01
Ext. std	3633	3665	-0.9%	-5.79	0.01	-3.59	0.02
Ext. std	2952	3180	-7.2%	-36.71	0.01	-9.81	0.03
Ext. std	5061	5380	-5.9%	-36.70	0.01	-9.52	0.01

103

APPENDIX I: DOLOMITE STABLE ISOTOPE ANALYSIS

Sample Notes: Northcoast dolomites P.R.

Data File: 080410_KIEL_GC_M.Torres_Northcoast P.R._a

Identifier 2	1 Cycle Int Samp 44	1 Cycle Int Ref 44	Δ mV	δ ^{13}C VPDB	δ^{13}C/^{12}C Std Dev	δ ^{18}O VPDB	δ^{18}O/^{16}O Std Dev
Ext. std	2747	2755	-0.3%	-36.26	0.00	-9.64	0.02
Ext. std	4056	4195	-3.3%	-35.55	0.01	-15.98	0.01
Ext. std	2473	2534	-2.4%	-35.50	0.01	-16.15	0.01
Ext. std	2785	2891	-3.7%	-35.46	0.01	-16.04	0.01
Ext. std	2225	2249	-1.1%	-3.84	0.01	-7.76	0.03
Ext. std	3060	3070	-0.3%	-4.01	0.01	-7.56	0.01
Ext. std	2313	2347	-1.4%	-3.69	0.01	-7.45	0.02
Ext. std	2728	2796	-2.4%	-3.97	0.00	-7.71	0.02

APPENDIX I: DOLOMITE STABLE ISOTOPE ANALYSIS

Analyzed by:	Greg Cane			**For P.I. / Institution:**	María Torres				
Analysis Date:	4/11/2008			**Sample Notes:**	Northcoast dolomites P.R.				
				Data File:	080411_KIEL_GC_M.Torres_Northcoast P.R._b				

Date	Identifier 1	Identifier 2	1 Cycle Int Samp 44	1 Cycle Int Ref 44	Δ mV	δ ^{13}C VPDB	δ^{13}C/^{12}C Std Dev	δ ^{18}O VPDB	δ^{18}O/^{16}O Std Dev
04/11/08	BCB.03.03.A-1.A		3146	3156	-0.3%	-10.69	0.02	-3.44	0.01
04/11/08	1513-02	calcite	2503	2556	-2.1%	1.40	0.01	1.68	0.01
04/11/08	1513-03	dolomite	2499	2530	-1.2%	1.10	0.01	1.29	0.00
04/11/08	1513-04	dolomite	2328	2321	0.3%	1.55	0.01	1.46	0.01
04/11/08	1513-05	calcite	2033	2066	-1.6%	1.08	0.02	1.20	0.01
04/11/08	1378-06	dolomite	3569	3640	-2.0%	0.88	0.01	2.04	0.01
04/11/08	1378-07	dolomite	2701	2726	-0.9%	1.06	0.01	1.73	0.02
04/11/08	1378-08	dolomite	2969	2958	0.4%	0.86	0.01	1.88	0.01
04/11/08	1378-09	calcite	3291	3302	-0.3%	0.76	0.00	1.85	0.02
04/11/08	1378-10	calcite	3471	3496	-0.7%	0.83	0.00	1.85	0.01
04/11/08	1378-11	dolomite	3029	3102	-2.4%	0.94	0.01	1.95	0.02
04/11/08	1378-12	dolomite	3453	3611	-4.4%	1.04	0.01	1.96	0.02
04/12/08	1708-13	dolomite	2533	2591	-2.2%	-8.94	0.01	0.09	0.01
04/12/08	1708-14	calcite	3685	3837	-4.0%	-7.18	0.00	-0.79	0.01
04/12/08	1708-15	dolomite	3376	3357	0.6%	-9.77	0.01	0.35	0.02
04/12/08	1708-16	dolomite	3871	4058	-4.6%	-8.16	0.00	-0.07	0.01
04/12/08	1708-17	dolomite	2252	2252	0.0%	-7.99	0.01	-0.01	0.02
04/12/08	1671-18	dolomite	2054	2060	-0.3%	1.45	0.01	1.42	0.02
04/12/08	1671-19	calcite	3900	4051	-3.7%	1.48	0.01	1.67	0.02
04/12/08	1671-20	dolomite	1680	1694	-0.8%	1.37	0.01	1.18	0.04
04/12/08	1671-21	calcite	1879	1902	-1.2%	1.33	0.01	1.16	0.02
04/12/08	1671-22	dolomite	1557	1568	-0.7%	0.98	0.01	0.92	0.01
04/12/08	1378-23	dolomite	3300	3346	-1.4%	1.19	0.01	1.54	0.02
04/12/08	1378-24	calcite	4305	4513	-4.6%	1.20	0.01	1.63	0.02
04/12/08	1378-25	dolomite	3077	3052	0.8%	1.09	0.01	1.68	0.01
04/12/08	1378-26	dolomite	2521	2548	-1.1%	0.72	0.01	2.02	0.01
04/12/08	1378-27	dolomite	2967	2984	-0.6%	0.89	0.01	1.80	0.01
04/12/08	1715-28	calcite	4040	4067	-0.7%	-6.65	0.01	-4.32	0.02
04/12/08	1715-29	calcite	3102	3193	-2.8%	-6.33	0.01	-4.64	0.01
04/12/08	1715-30	calcite	3314	3438	-3.6%	-6.89	0.01	-4.35	0.01
04/12/08	1715-31	calcite	3769	3775	-0.2%	-6.13	0.02	-4.79	0.02
04/12/08	1715-32	calcite	3769	3767	0.1%	-6.90	0.01	-4.40	0.02
04/12/08	1715b-33	calcite	2932	3009	-2.6%	-6.94	0.00	-4.52	0.02
04/12/08	1715b-34	dolomite	2999	2993	0.2%	-6.67	0.01	-4.59	0.01
04/12/08	1715b-35	dolomite	3371	3458	-2.5%	-7.06	0.01	-4.73	0.01
04/12/08	1715b-36	calcite	2963	2957	0.2%	-6.83	0.01	-4.44	0.03
04/12/08	1715c-37	calcite	2896	2898	-0.1%	-6.81	0.01	-4.82	0.01
04/12/08	1715c-38	calcite	3328	3354	-0.8%	-6.43	0.01	-4.30	0.02
04/12/08	1715c-39	calcite	2377	2391	-0.6%	-6.66	0.01	-4.26	0.02
04/12/08	1715c-40	dolomite	2655	2709	-2.0%	-7.20	0.02	-4.84	0.01

APPENDIX II: STABLE ISOTOPES VALUES OF DOLOMITES FROM (RAMÍREZ, 2000)

Stable Isotopes in Dolomites

(bulk samples)

Sample	Depth (m)	$\delta^{18}O$	$\delta^{13}C$	Strat. Unit
NC-6	707.6	+0.50	-1.13	Undif. Cibao Fm.
IAS-4	420.1	+1.76	+0.29	Montebello Mem.
	461.3	-0.61	-0.38	Montebello Mem.
	510.1	+1.42	+0.35	Montebello Mem.
	510.1 A	+1.20	+0.10	Montebello Mem.
	556.4	+1.71	+0.17	Lares Fm.
	563.1	+1.55	+0.75	Lares Fm.
	590.5	+0.53	+0.20	Lares Fm.
GAR	636.3	+0.74	+1.73	Lares Fm.
	653.0	+0.74	+1.74	Lares Fm.
	714.9	+0.58	+1.71	Lares Fm.
	718.3	+0.77	+1.60	Lares Fm.
	743.9	+0.06	+1.24	Lares Fm.
NC-10	430.8	+1.56	+0.18	Montebello Mem.
	430.8 A	+1.91	+0.20	Montebello Mem.
NC-5	387.8	+0.90	-1.43	Montebello Mem.
	387.8 A	+1.16	-1.00	Montebello Mem.
	520.7	+1.45	+0.57	Lares Fm.
IAS-1	420.1	+1.35	+0.98	Undif. Cibao Fm.
	612.8	-0.08	+2.43	Lares Fm.
	679.9	+0.12	-0.22	Lares Fm.
	685.7	+0.03	+0.16	Lares Fm.
NC-9	477.4	+0.17	-3.86	Lares Fm.
	493.0	+0.05	-1.51	Lares Fm.
	525.3	+2.18	+1.20	Lares Fm.

106

APPENDIX III: STRONTIUM ISOTOPES VALUES OF DOLOMITES FROM (RAMÍREZ, 2000)

$^{87}Sr/^{86}Sr$ Isotopic Ratios in Puerto Rico Dolomites,
Igneous Rocks and Groundwaters

Sample	Depth (m) (or sample location)	$^{87}Sr/^{86}Sr$ Ratio
NC-5 [1]	387.8	0.708509
IAS-1 [1]	679.9	0.708364
IAS-1 [1]	685.7	0.708276
Gar [1]	714.9	0.708286
IAS-4 [1]	510.1	0.708326
DAZI #2 [2]	Barceloneta	0.708295
Tiburón #2 [2]	Barceloneta	0.708288
DPI #3 [2]	Arecibo	0.708265
Florida #3 [2]	Florida	0.708211
Florida #3 [2]	Florida	0.708199
Camuy GW [3]	Camuy Cave	0.7082
Island Basalts [4]	Cental P.R.	0.703236 - 0.705746
Utuado Pluton A [5]	Utuado	0.70350
Utuado Pluton B [5]	Utuado	0.70367
Morovis stock [5]	Morovis	0.70415

1 this study: dolomites analyzed at the University of Texas at Austin
2 this study: aquifer waters analyzed at the University of Texas at Austin
3 from: Jay Banner at the University of Texas at Austin (personal communication, 1998)
4 from: Jolly et al., 1998
5 from: Frost et al., 1998

APPENDIX IV: IRON AND MAGNESE CONCENTRATIONS IN DOLOMITES FROM (RAMÍREZ, 2000)

Core/depth (m)	Fe	Mn
IAS4 -420.1 A	95.1	19.9
IAS4 -420.1 B	100.0	18.1
IAS4 -461.3	169.5	25.4
IAS4 -510.1 A	624.8	17.2
IAS4 -510.1 B	381.0	16.8
IAS4 -556.4	658.2	19.6
IAS4 -590.5	147.3	8.7
GAR -636.3	3.7	7.1
GAR -653	0.0	9.2
GAR -714.9	149.3	8.5
GAR -718.3	88.8	9.1
GAR -743.9	471.6	18.7
NC10 -430.8 A	126.4	35.6
NC10 -430.8 B	74.3	29.6
NC5 -387.8 A	153.0	19.2
NC5 -387.8 B	157.2	17.3
NC5 -520.3	845.8	22.5
IAS1 -679.9	255.4	67.3
IAS1 -685.7 A	298.3	24.0
IAS1 -685.7 B	259.1	20.5
NC9 -525.3 A	363.0	100.1
NC9 -525.3 B	276.6	99.2

APPENDIX V: ELEMENTAL CONCENTRATION IN DOLOMITES
Elemental Concentrations in Dolomites (RAMÍREZ, 2000)

Sample	Depth(m)	Ca	Mg	Fe	Mn	Si	Al	Sr	Na
IAS-4	420.1	256500	128800	100.0	18.1	248.7	101.0	339.9	273.6
	461.3	302000	146600	169.5	25.4	635.7	313.1	418.2	326.9
	510.1	268600	131100	624.8	17.2	954.9	439.8	364.4	252.2
	510.1	272600	132200	381.0	16.8	1087.7	410.1	355.2	307.5
	556.4	261600	127500	658.2	19.6	2004.5	673.1	342.6	321.6
GAR	653.0	294200	137100	0.000	9.2	240.9	99.4	430.0	303.5
	714.9	265500	129100	149.3	8.5	349.4	143.9	335.6	183.3
	718.3	275600	133900	88.80	9.1	331.7	167.7	353.4	228.7
	743.9	286700	139700	471.6	18.7	2101.5	583.3	349.7	334.3
NC-10	430.8	292900	143600	126.4	35.6	78.7	162.8	384.2	299.5
	430.8	250900	124300	74.30	29.6	42.7	134.3	324.2	209.3
NC-5	387.8	288500	139900	153.0	19.2	171.1	314.7	304.2	252.8
	387.8	247900	120600	157.2	17.3	332.8	255.7	260.1	243.5
	520.7	279600	137900	845.8	22.5	2504.9	875.0	351.4	360.6
IAS-1	679.9	275100	133200	255.4	67.3	401.5	160.9	358.3	203.0
	685.7	271800	129900	259.1	20.5	232.2	173.4	447.8	255.8
NC-9	525.3	293900	141500	276.6	99.2	295.5	394.8	408.3	224.8

Elemental Concentrations in Dolomites
(results in ppm)